

Walking in the Shadow: A New Perspective on Descent Directions for Constrained Minimization

Hassan Mortagy¹, Swati Gupta¹, and Sebastian Pokutta²

¹Georgia Institute of Technology
{hmortagy,swatig}@gatech.edu

²Zuse Institute Berlin and Technische Universität Berlin
pokutta@zib.de

Abstract

Descent directions such as movement towards Descent directions, including movement towards Frank-Wolfe vertices, away-steps, in-face away-steps and pairwise directions, have been an important design consideration in conditional gradient descent (CGD) variants. In this work, we attempt to demystify the impact of the movement in these directions towards attaining constrained minimizers. The optimal local direction of descent is the directional derivative (i.e., shadow) of the projection of the negative gradient. We show that this direction is the best away-step possible, and the continuous-time dynamics of moving in the shadow is equivalent to the dynamics of projected gradient descent (PGD), although it's non-trivial to discretize. We also show that Frank-Wolfe (FW) vertices correspond to projecting onto the polytope using an “infinite” step in the direction of the negative gradient, thus providing a new perspective on these steps. We combine these insights into a novel Shadow-CG method that uses FW and shadow steps, while enjoying linear convergence, with a rate that depends on the number of breakpoints in its projection curve, rather than the pyramidal width. We provide a linear bound on the number of breakpoints for simple polytopes and present scaling-invariant upper bounds for general polytopes based on the number of facets. We exemplify the benefit of using Shadow-CG computationally for various applications, while raising an open question about tightening the bound on the number of breakpoints for general polytopes.

1 Introduction

We consider the optimization problem $\min_{x \in \mathcal{P}} h(x)$, where $\mathcal{P} \subseteq \mathbb{R}^n$ is a polytope, and $h : \mathcal{P} \rightarrow \mathbb{R}$ is a differentiable, smooth, and strongly convex function. Smooth convex optimization problems over polytopes represent an important class of optimization problems encountered in various settings, such as low-rank matrix completion [1], structured supervised learning [2, 3], electrical flows over graphs [4], video co-localization in computer vision [5], traffic assignment problems [6], and submodular

function minimization [7]. First-order methods in convex optimization rely on movement in the best local direction for descent (e.g., negative gradient), and this is enough to obtain linear convergence for unconstrained optimization. However, in constrained settings, the gradient may no longer be a feasible direction of descent, and there are two broad classes of methods traditionally: (i) projection-based methods that move in the direction of the negative gradient and then project to ensure feasibility, and (ii) conditional gradient methods that move in feasible directions which approximate the gradient. Projection-based methods such as projected gradient descent or mirror descent [8] enjoy dimension independent linear rates of convergence (assuming no acceleration), for instance, $(1 - \frac{\mu}{L})$ contraction in the objective per iteration (so that the number of iterations to get an ϵ -accurate solution is $O(\frac{L}{\mu} \log \frac{1}{\epsilon})$), for μ -strongly convex and L -smooth functions, but need to compute an expensive projection step (another constrained convex optimization) in (almost) every iteration. On the other hand, conditional gradient methods (such as the Frank-Wolfe algorithm [9]) solely rely on solving linear optimization (LO) problems in every iteration and the rates of convergence become dimension-dependent, e.g., the away-step Frank-Wolfe algorithm has a linear rate of $(1 - \frac{\mu\rho^2}{LD^2})$, where ρ is a polytope dependent geometric constant and D is the diameter of the polytope [10].

The standard Conditional Gradient method (CG) or the Frank-Wolfe algorithm (FW) [9, 11] has received a lot of interest from the ML community mainly because of its iteration complexity, tractability and sparsity of iterates. In each iteration, the CG algorithm computes the *Frank-Wolfe vertex* $v^{(t)}$ with respect to the current iterate and moves towards that vertex:

$$v^{(t)} = \arg \min_{v \in \mathcal{P}} \langle \nabla h(x^{(t)}), v \rangle, \quad x^{(t+1)} = x^{(t)} + \gamma_t(v^{(t)} - x^{(t)}), \quad \gamma_t \in [0, 1].$$

CG's primary direction of descent is $v^{(t)} - x^{(t)}$ (d_t^{FW} in Figure 1) and its step-size γ_t can be selected, e.g., using line-search; this ensures feasibility of x_{t+1} . The FW algorithm however, can only guarantee a sub-linear rate of convergence $O(1/t)$ for smooth and strongly convex optimization on a polytope [9, 2]. Moreover, this convergence rate is tight [12, 13]. An active area of research, therefore, has been to find other descent directions that can enable linear convergence. One reason for the standard CG's $O(1/t)$ rate is the fact that the algorithm might zig-zag as it approaches the optimal face, slowing down progress [10, 12]. The key idea for obtaining linear convergence was to use the so-called *away-steps* that help push iterates to the optimal face:

$$\begin{aligned} a^{(t)} &= \arg \max_{v \in F} \langle \nabla h(x^{(t)}), v \rangle, \quad \text{for } F \subseteq \mathcal{P}, \\ x^{(t+1)} &= x^{(t)} + \gamma_t(x^{(t)} - a^{(t)}), \quad \text{where } \gamma_t \in \mathbb{R}_+ \text{ such that } x^{(t+1)} \in \mathcal{P}, \end{aligned} \tag{1}$$

thus, augmenting the potential directions of descent using directions of the form $x^{(t)} - a^{(t)}$, for some $a^{(t)} \in F$, where the precise choice of F in (1) has evolved in CG variants.

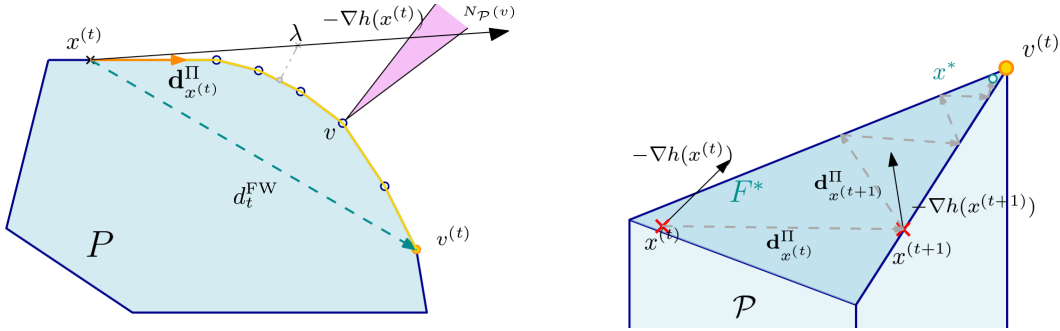


Figure 1: Left: Piecewise linearity of the parametric projections curve $g(\lambda) = \Pi_{\mathcal{P}}(x^{(t)} - \lambda \nabla h(x^{(t)}))$ (yellow line). The end point is the FW vertex $v^{(t)}$ and d_t^{FW} is the FW direction. Note that $g(\lambda)$ does not change at the same speed as λ , e.g., $g(\lambda) = v$ for each λ such that $x^{(t)} - \lambda \nabla h(x^{(t)}) - v \in N_{\mathcal{P}}(v)$ (purple normal cone). Right: Moving along the shadow as defined in (2) might lead to arbitrarily small progress even once we reach the optimal face $F^* \ni x^*$. On the contrary, the away-step FW algorithm does not leave F^* after a polytope-dependent iteration [14].

1.1 Related Work and Key Open Question:

As early as 1986, Guélat and Marcotte showed that by adding away-steps (with $F =$ minimal face of the current iterate^{*}) to vanilla CG, their algorithm has an asymptotic linear convergence rate [14]. In 2015, Lacoste-Julien and Jaggi [10] showed linear convergence results for CG with away-steps[†] (over $F =$ convex hull of the current active set, i.e., a specific convex decomposition of the current iterate). They also showed a linear rate of convergence for CG with pairwise-steps (of the form $v^{(t)} - a^{(t)}$), another direction of descent. In 2015, Freund et. al [1] showed an $O(1/t)$ convergence for convex functions, with F as the minimal face of the current iterate. In 2016, Garber and Meshi [16] showed that pairwise-steps (over 0/1 polytopes) with respect to non-zero components of the gradient are enough for linear convergence, i.e., they also set F to be the minimal face with respect to $x^{(t)}$. In 2017, Bashiri and Zhang [3] generalized this result to show linear convergence for the same F for general polytopes (at the cost of two expensive oracles however).

Other related research includes linear convergence for the conditional gradient method over strongly-convex domains with a lower bound on the norm of the optimum gradient [11], or when the FW-vertex is constrained to a ball around the iterate [13, 16], bringing in regularization-like ideas of mirror-descent variants to CG. There has also been extensive work on mixing Frank-Wolfe and gradient descent steps [17] or solving projections approximately using Frank-Wolfe steps [18] (with the aim of better computational performance) while enjoying linear convergence [18, 17]. Our objective in this study is to contextualize these CG variants and elucidate the properties of various feasible descent directions.

Although all these variants obtain linear convergence, their rates depend on polytope-dependent geometric, affine-variant constants (that can be arbitrarily small for non-polyhedral sets like the ℓ_2 -ball) such as the pyramidal-width [10], vertex-facet distance [19], or sparsity-dependent constants

^{*}The minimal face F with respect to $x^{(t)}$ is a face of the polytope that contains $x^{(t)}$ in its relative interior, i.e., all active constraints at $x^{(t)}$ are tight.

[†]To the best of our knowledge, Garber and Hazan [15] were the first to present a CG variant with global linear convergence for polytopes.

[3], which have been shown to be essentially equivalent [20]. The iterates in CG algorithms are (basically) affine-invariant; this underpins the inevitability of a dimension-dependent factor in current discussions. Following our work, there have been recent results on extensions using procedures similar to our TRACE-OPT procedure to avoid “bad” steps in CG variants and obtain linear convergence rates that depend on a slope condition rather than geometric constants [21, 22], and using shadow directions to speed up FW algorithms [23].

Key Open Question: A natural question at this point is why are these different descent directions useful and which of these are necessary for linear convergence. If one had oracle access to the “best” local direction of descent for constrained minimization, what would it be and is it enough to obtain linear convergence like in unconstrained optimization? Additionally, can we circumvent convergence rates contingent upon the polytope’s geometry, e.g., using affine-variant constants like pyramidal width? We partially answer these questions below.

1.2 Contributions

We show that the “best” local feasible direction of descent, giving the maximum function value decrease in the diminishing neighborhood of the current iterate $x^{(t)}$, is the *directional derivative* $d_{x^{(t)}}^{\Pi}$ of the projection of the gradient, which we call the *shadow* of the gradient:

$$d_{x^{(t)}}^{\Pi} := \lim_{\epsilon \downarrow 0} \frac{\Pi_{\mathcal{P}}(x^{(t)} - \epsilon \nabla h(x^{(t)})) - x^{(t)}}{\epsilon}, \quad (2)$$

where $\Pi_{\mathcal{P}}(y) = \arg \min_{x \in \mathcal{P}} \|x - y\|^2$ is the Euclidean projection operator. Further, a continuous time dynamical system can be defined using infinitesimal movement in the shadow direction at the current point: $\dot{X}(t) = d_{X(t)}^{\Pi}$, with $X(0) = x^{(0)} \in \mathcal{P}$. We show that this ODE is equivalent to that of projected gradient descent (Theorem 8), but is non-trivial to discretize due to non-differentiability of the curve.

Second, we explore structural properties of shadow steps. For any $x \in \mathcal{P}$, we characterize the curve $g(\lambda) = \Pi_{\mathcal{P}}(x - \lambda \nabla h(x))$ as a piecewise linear curve, where the breakpoints of the curve typically occur at points where there is a change in the normal cone (Theorem 2) and show how to compute this curve for all $\lambda \geq 0$ (Theorem 3). The projections curve is piecewise linear, as can be shown using parametric complementary pivot theory [24, 25]. Existing pivoting algorithms often inefficiently search for a basic feasible solution (BFS) of the KKT conditions at each breakpoint to find the next linear segment. In contrast, we characterize the entire projections curve by showing that it consists of two directions: the shadow of the negative gradient and its in-face shadow. We show that these directions can be computed in $O(n)$ time for the hypercube (Equation (13)) and in $O(n^2)$ for the simplex (Lemma 4), which subsequently allows us to compute the entire projections curve for the hypercube and simplex in $O(n^2)$ and $O(n^3)$ time respectively.

Additionally, we show the following properties for descent directions:

(i) Shadow Steps ($d_{x^{(t)}}^\Pi$): These represent the best *normalized feasible directions* of descent (Lemma 5). Moreover, we show that $\|d_{x^{(t)}}^\Pi\| = 0$ is a true measure of primal optimality gaps (in constrained optimization) without any dependence on geometric constants like those used in other CG variants (Lemma 6): (i) $\|d_{x^{(t)}}^\Pi\| = 0$ if and only if $x^{(t)} = \arg \min_{x \in \mathcal{P}} h(x)$; (ii) for μ -strongly convex functions, we show that $\|d_{x^{(t)}}^\Pi\|_2^2 \geq 2\mu(h(x^{(t)}) - h(x^*))$, which generalizes the well known PL inequality [26]. We show that multiple shadow steps approximate a single projected gradient descent step (Theorem 3). The rate of linear convergence using shadow steps is dependent on the number of facets (independent of geometric constants but dimension dependent due to the number of facets), and *interpolate smoothly* between projected gradient and conditional gradient methods (Theorem 10).

(ii) FW-Steps ($v^{(t)} - x^{(t)}$): Projected gradient steps provide a contraction in the objective, independent of the geometric constants or the polytope’s facets; they correspond to the maximum descent (in terms of distance between points) that one can obtain on the polytope, by taking unconstrained gradient steps and then projecting back to the polytope. Under mild technical conditions (uniqueness of $v^{(t)}$), we show that the Frank-Wolfe vertices are in fact the projection of an infinite descent in the negative gradient direction (Theorem 7). This enables CG methods to greedily descend on the polytope maximally, compared to PGD methods, thereby providing a fresh perspective on FW-steps.

(iii) Away-Steps ($x^{(t)} - a^{(t)}$): Shadow steps are the *best normalized away-direction* with steepest local descent (Lemma 5). Shadow steps are in general convex combinations of potential active vertices minus the current iterate (Lemma 7) and therefore loose combinatorial properties such as dimension drop in active sets [3]. Shadow steps can visit the same face multiple times in a zig-zagging manner, see Figure 1 (right) for an example, unlike away-steps that use vertices and have a monotone decrease in dimension when they are consecutive.

(vi) Pairwise Steps ($v^{(t)} - a^{(t)}$): The progress in CG variants is bounded crucially using the inner product of the descent direction with the negative gradient. In this sense, pairwise steps are simply the *sum of the FW-step and “away” directions*, and a simple algorithm, the pairwise-FW algorithm, that only uses these steps does converge linearly (with geometric constants) [10, 3]. Moreover, for feasibility of the descent direction, one requires $a^{(t)}$ to be in the active set of the current iterate (shown in Lemma 8).

Armed with these structural properties, we consider a descent algorithm SHADOW-WALK. It traces the projections curve by moving in the shadow or an in-face directional derivative with respect to a fixed iterate, until sufficient progress is achieved, and then updates the shadow based on the current iterate. Using properties of normal cones, we can show that once the projections curve at a fixed iterate leaves a face, it can never visit the face again (Theorem 4). We are thus able to break a single PGD step into multiple descent steps, and show linear convergence with rate dependent on the number of facets, but independent of geometric constants like the pyramidal-width.

We combine these insights into a novel SHADOW-CG method which uses FW-steps and shadow steps (both over the tangent cone and minimal face), while enjoying linear convergence. This method prioritizes FW-steps that achieve maximal “coarse” progress in earlier iterations and shadow steps avoid zig-zagging in the latter iterations. Garber and Meshi [16] and Bashiri and Zhang [3] both compute the best away vertex in the minimal face containing the current iterate, whereas the shadow step recovers the best convex combination of such vertices aligned with the negative gradient. Therefore, these previously mentioned CG methods can *both* be viewed as approximations of SHADOW-CG. Moreover, Garber and Hazan [15] emulate a shadow computation by constraining the FW vertex to a ball around the current iterate. Therefore, their algorithm can be interpreted as an approximation of SHADOW-WALK. We further show that SHADOW-WALK and SHADOW-CG achieve a factor of $\Omega(n)$ reduction in iteration complexity over the simplex, and an overall $\Omega(n^2)$ reduction in running time over the hypercube, compared to AFW. Finally, we propose a practical variant of SHADOW-CG, called SHADOW-CG², which reduces the number of shadow computations.

Outline. We next review preliminaries in Section 2. In Section 3, we derive theoretical properties of the piecewise-linear projections curve and prove that the number of breakpoints of the projections curve $g(\lambda)$ is $O(n)$ for both the simplex and the hypercube. Next, we derive properties of descent directions in Section 4 and present the continuous time dynamics for movement along the shadow and its discretization SHADOW-WALK in Section 5. We propose SHADOW-CG and SHADOW-CG² in Section 6, and benchmark our algorithms against AFW. Finally, we provide computational experiments in Section 7.

2 Preliminaries

Let $\|\cdot\|$ denote the Euclidean norm and let $\mathcal{P} \subseteq \mathbb{R}^n$ denote a polytope defined in the form

$$\mathcal{P} = \{x \in \mathbb{R}^n : \langle a_i, x \rangle \leq b_i \forall i \in [m]\}. \quad (3)$$

We use $\text{vert}(\mathcal{P})$ to denote the vertex set of \mathcal{P} . A function $h : \mathcal{P} \rightarrow \mathbb{R}$ is said to be L -smooth if $h(y) \leq h(x) + \langle \nabla h(x), y - x \rangle + \frac{L}{2} \|y - x\|^2$ for all $x, y \in \mathcal{P}$. Furthermore, $h : \mathcal{P} \rightarrow \mathbb{R}$ is said to be μ -strongly-convex if $h(y) \geq h(x) + \langle \nabla h(x), y - x \rangle + \frac{\mu}{2} \|y - x\|^2$ for all $x, y \in \mathcal{P}$. Let $D := \sup_{x, y \in \mathcal{P}} \|x - y\|$ be the diameter of \mathcal{P} . We let $x^* = \arg \min_{x \in \mathcal{P}} h(x)$, where uniqueness follows from the strong convexity of the h . For any $x \in \mathcal{P}$, we let $I(x) = \{i \in [m] : \langle a_i, x \rangle = b_i\}$ be the index set of active constraints at x . Similarly, let $J(x)$ be the index set of inactive constraints at x . Denote by $A_{I(x)} = [a_i]_{i \in I(x)}$ the sub-matrix of active constraints at x and $b_{I(x)} = [b_i]_{i \in I(x)}$ the corresponding right-hand side. The normal cone at a point $x \in \mathcal{P}$ is defined as

$$N_{\mathcal{P}}(x) := \{y \in \mathbb{R}^n : \langle y, z - x \rangle \leq 0 \forall z \in \mathcal{P}\} = \{y \in \mathbb{R}^n : \exists \mu : y = \mu^\top A_{I(x)}, \mu \geq 0\}, \quad (4)$$

which is essentially the cone of the normals of constraints tight at x . The *tangent cone* at a point $x \in \mathcal{P}$ is defined as

$$T_{\mathcal{P}}(x) := \{d \in \mathbb{R}^n : A_{I(x)}d \leq 0\}, \quad (5)$$

that is $T_{\mathcal{P}}(x) = \text{cone}(\mathcal{P} - x)$ is the cone of feasible directions in \mathcal{P} from x .

We next review some results on Euclidean projections over polytopes that we will use in this paper. Let $\Pi_{\mathcal{P}}(y) = \arg \min_{x \in \mathcal{P}} \frac{1}{2} \|x - y\|^2$ be the *Euclidean projection operator*. Using first-order optimality, we have $x^* = \Pi_{\mathcal{P}}(y)$ if and only if

$$\langle y - x, z - x \rangle \leq 0 \quad \forall z \in \mathcal{P} \quad \iff \quad (y - x) \in N_{\mathcal{P}}(x). \quad (6)$$

It is well known that the Euclidean projection operator over convex sets is non-expansive (see e.g., [27]): $\|\Pi_{\mathcal{P}}(y) - \Pi_{\mathcal{P}}(x)\| \leq \|y - x\|$ for all $x, y \in \mathbb{R}^n$. Given any point $x \in \mathcal{P}$ and $w \in \mathbb{R}^n$, let the *directional derivative* of w at x be defined as (note it is the projection of $-w$ direction onto the tangent cone at x for brevity of results):

$$d_x^{\Pi}(w) := \lim_{\epsilon \downarrow 0} \frac{\Pi_{\mathcal{P}}(x - \epsilon w) - x}{\epsilon}. \quad (7)$$

When $w = \nabla h(x)$, then we call $d_x^{\Pi}(\nabla h(x))$ the *shadow of the negative gradient* at x , and use notation d_x^{Π} for brevity. In [28], Tapia et. al show that d_x^{Π} is the projection of $-\nabla h(x)$ onto the tangent cone at x : $d_x^{\Pi} = \arg \min_{d \in T_{\mathcal{P}}(x)} \{\|-\nabla h(x) - d\|^2\} = \arg \min_{d \in \mathbb{R}^n} \{\|-\nabla h(x) - d\|^2 : A_{I(x)}d \leq 0\}$, where the uniqueness of the solution follows from strong convexity of the objective. Further, let $\hat{d}_x^{\Pi}(\nabla h(x))$ be the projection of $-\nabla h(x)$ onto $\text{Cone}(F - x) = \{d \in \mathbb{R}^n : A_{I(x)}d = 0\}$, where F is the minimal face of P containing x^{\ddagger} . That is, $\hat{d}_x^{\Pi}(\nabla h(x))$ is the projection of $-\nabla f(x)$ onto the set of in-face feasible directions and can be computed in closed-form using: $\hat{d}_x^{\Pi}(\nabla h(x)) = \arg \min_{d \in \mathbb{R}^n} \{\|-\nabla h(x) - d\|^2 : A_{I(x)}d = 0\} = (I - A_{I(x)}^{\dagger} A_{I(x)})(-\nabla h(x))$, where $I \in \mathbb{R}^{n \times n}$ is the identity matrix, and $A_{I(x)}^{\dagger}$ is the Moore-Penrose inverse of $A_{I(x)}$ (see Section 5.13 in [29] for more details). We refer to $\hat{d}_x^{\Pi}(\nabla h(x))$ as the *in-face shadow* or *in-face directional derivative*.

We will also use the following Moreau's decomposition theorem in our analysis:

Theorem 1 (Moreau's Decomposition theorem [30]). *Let $\mathcal{K} \subseteq \mathbb{R}^n$ be a closed convex cone and let \mathcal{K}° be its polar cone, that is, the closed convex cone defined by $\mathcal{K}^{\circ} = \{y \in \mathbb{R}^n \mid \langle x, y \rangle \leq 0, \forall x \in \mathcal{K}\}$. Then, for $x, y, z \in \mathbb{R}^n$, the following statements are equivalent:*

(i) $z = x + y$, $x \in \mathcal{K}$, $y \in \mathcal{K}^{\circ}$, and $\langle x, y \rangle = 0$;

(ii) $x = \Pi_{\mathcal{K}}(z)$ and $y = \Pi_{\mathcal{K}^{\circ}}(z)$.

[‡]Note that $-(z - x)$ is also a feasible direction at x for any $z \in F$, since x is in the relative interior of F by definition. This implies that $\text{Cone}(F - x) = -\text{Cone}(F - x)$, and therefore $\text{Cone}(F - x)$ is in fact a subspace.

3 Structure of the Parametric Projections Curve

In this section, we characterize properties of the directional derivative at any $x \in \mathcal{P}$ and the structure of the parametric projections curve $g_{x,w}(\lambda) = \Pi_{\mathcal{P}}(x - \lambda w)$, for $\lambda \geq 0$, under Euclidean projections. For brevity, we use $g(\cdot)$ when x and w are clear from context. The following theorem summarizes our results and it is crucial to our analysis of descent directions:

Theorem 2 (Structure of Parametric Projections Curve). *Let $\mathcal{P} \subseteq \mathbb{R}^n$ be a polytope, with m facet inequalities (e.g., as in (3)). For any $x_0 \in \mathcal{P}, w \in \mathbb{R}^n$, let $g(\lambda) = \Pi_{\mathcal{P}}(x_0 - \lambda w)$ be the projections curve at x_0 with respect to w parametrized by $\lambda \in \mathbb{R}_+$. Then, this curve is piecewise linear starting at x_0 : there exist k breakpoints $x_1, x_2, \dots, x_k \in \mathcal{P}$, corresponding to projections with λ equal to $0 = \lambda_0^- \leq \lambda_0^+ < \lambda_1^- \leq \lambda_1^+ < \lambda_2^- \leq \lambda_2^+ \dots < \lambda_k^- \leq \lambda_k^+$, where*

(a) $\lambda_i^- := \min\{\lambda \geq 0 \mid g(\lambda) = x_i\}$, $\lambda_i^+ := \max\{\lambda \geq 0 \mid g(\lambda) = x_i\}$, for $i \geq 0$,

(b) $g(\lambda) = x_{i-1} + \frac{x_i - x_{i-1}}{\lambda_i^- - \lambda_i^+}(\lambda - \lambda_{i-1}^+)$, for $\lambda \in [\lambda_{i-1}^+, \lambda_i^-]$ for all $i \geq 1$.

Moreover, for each $1 \leq i \leq k$ and all $\lambda, \lambda' \in (\lambda_{i-1}^+, \lambda_i^-)$, the following hold:

- (i) **Potentially drop tight constraints on leaving breakpoints:** $N_{\mathcal{P}}(x_{i-1}) = N_{\mathcal{P}}(g(\lambda_{i-1}^+)) \supseteq N_{\mathcal{P}}(g(\lambda))$. Moreover, if $\lambda_{i-1}^- < \lambda_{i-1}^+$, then the containment is strict.
- (ii) **Constant normal cone between breakpoints:** $N_{\mathcal{P}}(g(\lambda)) = N_{\mathcal{P}}(g(\lambda'))$,
- (iii) **Potentially add tight constraints on reaching breakpoints:** $N_{\mathcal{P}}(g(\lambda)) \subseteq N_{\mathcal{P}}(g(\lambda_i^-)) = N_{\mathcal{P}}(x_i)$.

Further, the following properties also hold:

- (iv) **Equivalence of constant normal cones with linearity:** If $N_{\mathcal{P}}(g(\lambda)) = N_{\mathcal{P}}(g(\lambda'))$ for some $\lambda < \lambda'$, then the curve between $g(\lambda)$ and $g(\lambda')$ is linear (Lemma 2).
- (v) **Bound on breakpoints:** The number of breakpoints of $g(\cdot)$ is at most the number of faces of the polytope (Theorem 4).
- (vi) **Limit of $g(\cdot)$:** The end point of the curve $g(\lambda)$ is $\lim_{\lambda \rightarrow \infty} g(\lambda) = x_k \in \arg \min_{x \in \mathcal{P}} \langle x, w \rangle$. In fact, x_k minimizes $\|y - x_0\|$ over $y \in \arg \min_{x \in \mathcal{P}} \langle x, w \rangle$ (Theorem 7, Section 4).

To see an example of the projections curve, we refer the reader to Figure 2. Even though our results hold for any $w \in \mathbb{R}^n$, we will prove the statements for $w = \nabla h(x_0)$ for readability in the context of the chapter. Before we present the proof of Theorem 2, we first show that if $-\nabla h(x_0) \in N_{\mathcal{P}}(x_0)$, then $g(\lambda)$ reduces down to a single point x_0 .

Lemma 1. $g(\lambda) = \Pi_{\mathcal{P}}(x_0 - \lambda \nabla h(x_0)) = x_0$ for all $\lambda \in \mathbb{R}_+$ if and only if $-\nabla h(x_0) \in N_{\mathcal{P}}(x_0)$.

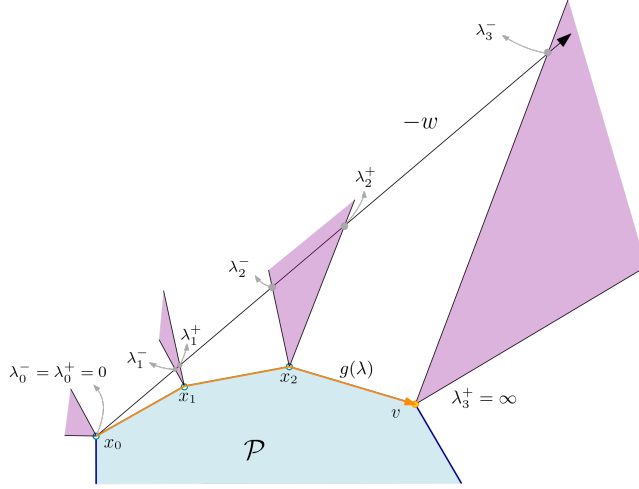


Figure 2: Figure showing the structure of the projections curve $g(\lambda) = \Pi_{\mathcal{P}}(x_0 - \lambda w)$ for $\lambda \geq 0$, which is depicted by the orange line. Breakpoints in the curve correspond to x_i with $g(\lambda_i^-) = g(\lambda_i^+) = x_i$, and $\lambda_3^+ = \infty$ since $\lim_{\lambda \rightarrow \infty} g(\lambda) = v = \arg \min_{y \in \mathcal{P}} \langle y, w \rangle$. Consider the first linear segment from x_0 to x_1 . We have $N_{\mathcal{P}}(g(\lambda)) = N_{\mathcal{P}}(g(\lambda')) \subset N_{\mathcal{P}}(x_0)$ for all $\lambda, \lambda' \in (0, \lambda_1^-)$. Then, another constraint becomes tight at the end point of the first segment x_1 , and thus we have $N_{\mathcal{P}}(g(\lambda)) \subset N_{\mathcal{P}}(x_1)$ for all $\lambda \in (0, \lambda_1^-)$. This process of dropping and adding constraints (given by Theorem 2(i) – (iii)) continues until we reach the endpoint v .

Proof. Note that $g(\lambda) = x_0$ if and only if x_0 satisfies the first order optimality condition for $g(\lambda)$: $\langle x_0 - \lambda \nabla h(x_0) - x_0, z - x_0 \rangle = \lambda \langle -\nabla h(x_0), z - x_0 \rangle \leq 0$ for all $z \in \mathcal{P}$. Since $\lambda \geq 0$, we can conclude that $g(\lambda) = x_0$ if and only if $\langle -\nabla h(x_0), z - x_0 \rangle \leq 0$ for all $z \in \mathcal{P}$. Note that $\langle -\nabla h(x_0), z - x_0 \rangle \leq 0$ for all $z \in \mathcal{P}$ is equivalent to saying that $-\nabla h(x_0) \in N_{\mathcal{P}}(x_0)$. \square

Thus, in the notation of Theorem 2, λ_0^+ is either infinity (when $-\nabla h(x_0) \in N_{\mathcal{P}}(x_0)$) or it is zero. In the former case, Theorem 2 holds trivially with $g(\lambda) = x_0$ for all $\lambda \in \mathbb{R}$. We will therefore assume that $\lambda_0^+ = 0$, without loss of generality.

We now show that the segment of the projections curve between two projected points with the same normal cones has to be linear (Theorem 2(iv)). This result will be crucial to bound on the number of breakpoints of the curve.

Lemma 2. *Let $\mathcal{P} \subseteq \mathbb{R}^n$ be a polytope. Let $x_0 \in \mathcal{P}$ and $\nabla h(x_0) \in \mathbb{R}^n$ be given. Let $g(\lambda) = \Pi_{\mathcal{P}}(x_0 - \lambda \nabla h(x_0))$ be the parametric projections curve. Then, if $N_{\mathcal{P}}(g(\lambda)) = N_{\mathcal{P}}(g(\lambda'))$ for some $\lambda < \lambda'$, then the curve between $g(\lambda)$ and $g(\lambda')$ is linear, i.e., $g(\delta\lambda + (1 - \delta)\lambda') = \delta g(\lambda) + (1 - \delta)g(\lambda')$, for $\delta \in [0, 1]$.*

Proof. We will show that the convex combination $\delta g(\lambda) + (1 - \delta)g(\lambda')$ of projections $g(\lambda)$ and $g(\lambda')$ satisfies the first-order optimality condition for the projection of $(x_0 - (\delta\lambda + (1 - \delta)\lambda') \nabla h(x_0))$, and is therefore equal to $g(\delta\lambda + (1 - \delta)\lambda')$. For brevity, let I and J denote the index set of active and inactive constraints at $g(\lambda)$ and $g(\lambda')$ (since the normal cones are assumed to be the same). The first-order optimality of $g(\lambda)$ and $g(\lambda')$ yields

$$x_0 - \lambda \nabla h(x_0) - g(\lambda) = \mu^\top A_I \in N_{\mathcal{P}}(g(\lambda)), \quad \text{for some } \mu \in \mathbb{R}_+^{|I|}, \quad (8)$$

$$x_0 - \lambda' \nabla h(x_0) - g(\lambda') = \tilde{\mu}^\top A_I \in N_P(g(\lambda)), \quad \text{for some } \tilde{\mu} \in \mathbb{R}_+^{|I|}. \quad (9)$$

Thus, by aggregating equations (8) and (9) with weights δ and $(1 - \delta)$ respectively, we get:

$$x_0 - (\delta\lambda + (1 - \delta)\lambda') \nabla h(x_0) - (\delta g(\lambda) + (1 - \delta)g(\lambda')) = (\delta\mu + (1 - \delta)\tilde{\mu})^\top A_I \in N_P(g(\lambda)). \quad (10)$$

But the normal cone $N_P(\delta g(\lambda) + (1 - \delta)g(\lambda')) = N_P(g(\lambda))$, since every point in the convex combination of two points with the same minimal face F must also have F as its minimal face. This proves the lemma. □

As an immediate corollary of this lemma we know that the projections curve does not intersect itself: if the projections curve leaves the a breakpoint x_i , then $g(\lambda') \neq x$ for all $\lambda' > \lambda_i + \epsilon$. Moreover, at any breakpoint of $g(\lambda)$, the normal cones must change (Theorem 2 (ii)). In addition, given any breakpoint x_i , we must drop constraints as soon as we leave x_i , i.e., $N_{\mathcal{P}}(g(\lambda_{i-1} + \epsilon)) \subseteq N_{\mathcal{P}}(x_{i-1})$ for $\epsilon > 0$ sufficiently small, since $g(\lambda_{i-1} + \epsilon) = x_i + \epsilon d$, where $d := \frac{g(\lambda_{i-1} + \epsilon) - x_i}{\epsilon} \in T_{\mathcal{P}}(x_i)$ is a feasible direction at x_i . Similarly, at the subsequent breakpoint x_{i+1} , there is a change in the normal cone, and therefore, new constraints must become tight (Theorem 2 (iii)). These structural properties of the projection curve can be formally derived using complementary pivot theory (see Appendix B for a reduction). However, these methods rely on finding the next basic feasible solution (BFS) of the KKT conditions, which can be very inefficient to compute the next segment of the curve. Instead, we give a polyhedral view of the projections curve, and algorithmically compute each of its segments as follows:

- (i) At a breakpoint x_i , if the shadow is orthogonal to normal of the projection at x_i , then the next linear segment of the projections curve is given by a maximal movement along the *shadow* direction;
- (ii) Otherwise, the next linear segment is obtained by moving along the “*in-face*” *shadow* direction until the normal cone changes.

Note that the only difference between the shadow and the in-face shadow is that the former projects the negative gradient onto the tangent cone at x (i.e., on $A_{I(x)}d \leq 0$), whereas the latter projects the negative gradient onto the minimal face of x (i.e., on $A_{I(x)}d = 0$). We formalize these movements below:

Theorem 3 (Breakpoints in the Projections Curve). *Let $\mathcal{P} \subseteq \mathbb{R}^n$ be a polytope. Let $x_{i-1} \in \mathcal{P}$ be the i th breakpoint in the projections curve $g(\lambda) = \Pi_{\mathcal{P}}(x_0 - \lambda \nabla h(x_0))$, with $x_{i-1} = x_0$ for $i = 1$. Let $\lambda_{i-1} \in \mathbb{R}_+$ be such that $g(\lambda_{i-1}) = x_{i-1}$. Then, if $d_{x_{i-1}}^\Pi(\nabla h(x_0)) = 0$, then $\lim_{\lambda \rightarrow \infty} g(\lambda) = x_{i-1}$ is the end point of $g(\lambda)$. Otherwise, $d_{x_{i-1}}^\Pi(\nabla h(x_0)) \neq 0$, in which case the following holds:*

[¶]This example is inspired by Damiano Zeffiro.

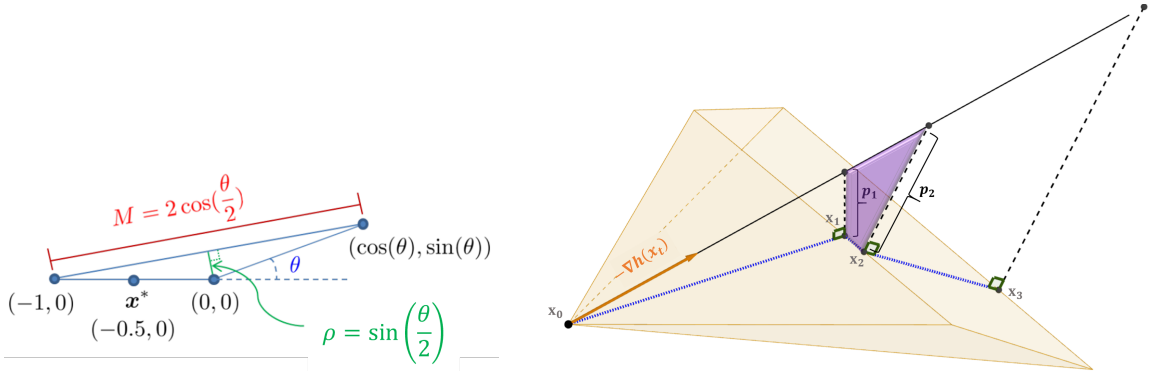


Figure 3: Left: Figure from Lacoste-Julien and Jaggi's work [10] showing the pyramidal-width δ of a simple triangle domain as a function of the angle θ . Right: An example of the projections curve, showing how the structure of the normal vectors $p_i := x_0 - \lambda_i \nabla h(x_0) - x_i$ determine whether we take an in-face step or shadow step[¶].

- (a) **Shadow steps:** If $\langle x_0 - \lambda_{i-1} \nabla h(x_0) - x_{i-1}, d_{x_{i-1}}^{\Pi}(\nabla h(x_0)) \rangle = 0$, then the next breakpoint of the projections curve can be obtained by moving maximally in the shadow direction, i.e.,

$$x_i := x_{i-1} + (\lambda_i^- - \lambda_{i-1}) d_{x_{i-1}}^{\Pi}(\nabla h(x_0)),$$

where $\lambda_i^- = \lambda_{i-1} + \max\{\delta : x_{i-1} + \delta d_{x_{i-1}}^{\Pi}(\nabla h(x_0)) \in \mathcal{P}\}$.

- (b) **In-face steps:** Otherwise, $\langle x_0 - \lambda_{i-1} \nabla h(x_0) - x_{i-1}, d_{x_{i-1}}^{\Pi}(\nabla h(x_0)) \rangle \neq 0$. Then, the next breakpoint is obtained by moving in the in-face direction until the normal cone changes, i.e.,

$$x_i := x_{i-1} + (\hat{\lambda}_{i-1} - \lambda_{i-1}) \hat{d}_{x_{i-1}}^{\Pi}(\nabla h(x_0)),$$

where $\hat{\lambda}_{i-1} := \sup\{\lambda \mid N_{\mathcal{P}}(g(\lambda')) = N_{\mathcal{P}}(x_{i-1}) \forall \lambda' \in [\lambda_{i-1}, \lambda]\}$.

We refer the reader to Figure 3 for an illustration of the theorem, and include this as an algorithm called TRACE (Algorithm 1). To prove this theorem, we first show that if at breakpoint x_{i-1} the shadow $d_{x_{i-1}}^{\Pi}(\nabla h(x_0)) = 0$, then x_{i-1} is the endpoint of the curve:

Lemma 3. *If the shadow $d_{x_{i-1}}^{\Pi}(\nabla h(x_0)) = 0$, then $\lim_{\lambda \rightarrow \infty} g(\lambda) = x_{i-1}$ is the end point of the projections curve $g(\lambda)$.*

Proof. Since $d_{x_{i-1}}^{\Pi}(\nabla h(x_0)) = 0$, using Moreau's decomposition theorem (see Theorem 1) we have $-\nabla h(x_0) \in N_{\mathcal{P}}(x_{i-1})$. Note that the first-order optimality condition of $g(\lambda_{i-1}) = x_{i-1}$ is $\langle p, z - x_{i-1} \rangle \leq 0$ for all $z \in \mathcal{P}$. Since $-\nabla h(x_0) \in N_{\mathcal{P}}(x_{i-1})$ (i.e., $\langle -\nabla h(x_0), z - x_{i-1} \rangle \leq 0 \forall z \in \mathcal{P}$) and $\lambda \geq \lambda_{i-1}$, we get $\langle x_0 - \lambda \nabla h(x_0) - x_{i-1}, z - x_{i-1} \rangle \leq 0 \forall z \in \mathcal{P}$. Thus, x_{i-1} satisfies the first-order optimality condition for $g(\lambda)$ when $\lambda \geq \lambda_{i-1}^+$. \square

We are now ready to prove Theorem 3:

Proof. Consider an ϵ -perturbation along the projections curve $g(\lambda_{i-1} + \epsilon)$ from x_{i-1} . Then, we can write $g(\lambda_{i-1} + \epsilon) = x_{i-1} + \epsilon d$ for some $d \in \mathbb{R}^n$, where $\epsilon > 0$ is sufficiently small. For brevity, let the

shadow at x_{i-1} be $d_{x_{i-1}}^\Pi := d_{x_{i-1}}^\Pi(\nabla h(x_0))$, and in-face shadow be $\hat{d}_{x_{i-1}}^\Pi := \hat{d}_{x_{i-1}}^\Pi(\nabla h(x_0))$. Define the normals of the projections $p_{i-1} := x_0 - \lambda_{i-1} \nabla h(x_0) - x_{i-1}$ and $p_\epsilon := x_0 - (\lambda_{i-1} + \epsilon) \nabla h(x_0) - g(\lambda_{i-1} + \epsilon)$ at x_{i-1} and $g(\lambda_{i-1} + \epsilon)$ respectively.

We now proceed with two cases:

- (a) Suppose that $\langle p_{i-1}, d_{x_{i-1}}^\Pi \rangle = 0$. In this case, we will prove that $d = d_{x_{i-1}}^\Pi$, by showing that $x_{i-1} + \epsilon d_{x_{i-1}}^\Pi$ satisfies first-order optimality for $g(\lambda_{i-1} + \epsilon)$. Indeed, for any $z \in \mathcal{P}$, we have

$$\begin{aligned} & \left\langle x_0 - (\lambda_{i-1} + \epsilon) \nabla h(x_0) - x_{i-1} - \epsilon d_{x_{i-1}}^\Pi, z - x_{i-1} - \epsilon d_{x_{i-1}}^\Pi \right\rangle \\ &= \left\langle p_{i-1} + \epsilon(-\nabla h(x_0) - d_{x_{i-1}}^\Pi), z - x_{i-1} - \epsilon d_{x_{i-1}}^\Pi \right\rangle \\ &= -\epsilon \underbrace{\langle p_{i-1}, d_{x_{i-1}}^\Pi \rangle}_{\stackrel{(i)}{=} 0} - \epsilon^2 \underbrace{\langle -\nabla h(x_0) - d_{x_{i-1}}^\Pi, d_{x_{i-1}}^\Pi \rangle}_{\stackrel{(ii)}{=} 0} \\ &+ \underbrace{\langle p_{i-1}, z - x_{i-1} \rangle}_{\stackrel{(iii)}{\leq 0}} + \epsilon \underbrace{\langle -\nabla h(x_0) - d_{x_{i-1}}^\Pi, z - x_{i-1} \rangle}_{\stackrel{(iv)}{\leq 0}} \leq 0, \end{aligned}$$

where we used our assumption $\langle p_{i-1}, d_{x_{i-1}}^\Pi \rangle = 0$ in (i), the definition of the shadow $d_{x_{i-1}}^\Pi := \Pi_{T_{\mathcal{P}}(x_{i-1})}(-\nabla h(x_0))$ in (ii), the first-order optimality at x_{i-1} in (iii), and the fact that $-\nabla h(x_0) - d_{x_{i-1}}^\Pi \in N_{\mathcal{P}}(x_{i-1})$ (by Moreau's decomposition theorem) in (iv).

Since the above argument holds for any ϵ such that $x_{i-1} + \epsilon d_{x_{i-1}}^\Pi \in \mathcal{P}$, it follows that the next breakpoint $x_i := x_{i-1} + (\lambda_i^- - \lambda_{i-1}) d_{x_{i-1}}^\Pi(\nabla h(x_0))$, where $\lambda_i^- = \lambda_{i-1} + \max\{\delta : x_{i-1} + \delta d_{x_{i-1}}^\Pi(\nabla h(x_0)) \in \mathcal{P}\}$. This proves case (a) in the theorem.

- (b) Now suppose that $\langle p_{i-1}, d_{x_{i-1}}^\Pi \rangle \neq 0$. We now show that in this case $d = \hat{d}_{x_{i-1}}^\Pi$. Since $g(\lambda_{i-1} + \epsilon) = x_{i-1} + \epsilon d$, by first-order optimality we have

$$\begin{aligned} & \langle x_0 - (\lambda_{i-1} + \epsilon) \nabla h(x_0) - x_{i-1} - \epsilon d, z - x_{i-1} - \epsilon d \rangle = -\epsilon \underbrace{\langle p_{i-1}, d \rangle}_{\stackrel{(i)}{=} 0} \\ & - \epsilon \underbrace{\langle -\nabla h(x_0) - d, \epsilon d \rangle}_{\stackrel{(ii)}{=} 0} + \underbrace{\langle p_{i-1}, z - x_{i-1} \rangle}_{\stackrel{(iii)}{\leq 0}} + \epsilon \langle -\nabla h(x_0) - d, z - x_{i-1} \rangle \leq 0 \quad \forall z \in \mathcal{P}, \quad (11) \end{aligned}$$

where we used the structure of orthogonal projections and the continuity of the projections curve which imply that $\langle p_\epsilon, d \rangle = 0$ and $\langle p_{i-1}, d \rangle = 0$ in (i). In (ii) we used the fact that $(p_\epsilon - p_{i-1})/\epsilon = -\nabla h(x_0) - d$, and thus taking the inner product with d on both sides implies that have $\langle d, -\nabla h(x_0) - d \rangle = 0$. We then used first-order optimality at x_{i-1} in (iii).

To analyze that last term in $\langle -\nabla h(x_0) - d, z - x_{i-1} \rangle$ in (11), we claim that $-\nabla h(x_0) = (-\nabla h(x_0) - d) \notin N_{\mathcal{P}}(x_i)$. To see this, suppose not. Since $\langle p_{i-1}, d \rangle = 0$, by Moreau's decomposition theorem (see Theorem 1) this implies that $d = d_{x_{i-1}}^\Pi$, which in turn implies that

$\langle p_{i-1}, d_{x_{i-1}}^{\Pi} \rangle = 0$, which is a contradiction to our assumption of case (b). Since $-\nabla h(x_0) - d \notin N_{\mathcal{P}}(x_{i-1})$, there exists a vertex $\tilde{z} \in \mathcal{P}$ such that $\langle -\nabla h(x_0) - d, \tilde{z} - x_{i-1} \rangle > 0$. Using (11) this must imply that $\langle p_{i-1}, \tilde{z} - x_{i-1} \rangle < 0$. However, first order optimality at x_{i-1} given by $\langle p_{i-1}, z - x_{i-1} \rangle \leq 0$ is a defining inequality for the face F , and hence satisfied with by all $z \in F$. Thus, $\tilde{z} \notin F$, which further implies that $\langle -\nabla h(x_0) - d, z - x_{i-1} \rangle \leq 0$ for all $z \in F$. This shows that $d = \hat{d}_{x_{i-1}}^{\Pi}$ as claimed, since it satisfies the first order optimality condition for $\hat{d}_{x_{i-1}}^{\Pi}$ as the projection of $-\nabla h(x_0)$ onto $\text{Cone}(F - x_{i-1})$ given by $\langle -\nabla h(x_0) - \hat{d}_{x_{i-1}}^{\Pi}, z - x_{i-1} \rangle \leq 0 \forall z \in F^{\parallel}$. Moreover, the next breakpoint $x_i := g(\hat{\lambda}_{i-1}) = x_{i-1} + (\hat{\lambda}_{i-1} - \lambda_{i-1})\hat{d}_{x_{i-1}}^{\Pi}$ by the definition of $\hat{\lambda}_{i-1}$ and the fact that the projections curve leaves the minimal face after this point, and thus direction change in the projections curve must happen by Lemma 2. This proves case (b) in the theorem. \square

We give an example of in TRACE in Figure 3-right. At the first breakpoint x_1 we have $\langle p_1, d_{x_1}^{\Pi}(\nabla h(x_0)) \rangle \neq 0$ in which case we take an in-face step, whereas at x_2 we have $\langle p_2, d_{x_2}^{\Pi}(\nabla h(x_0)) \rangle = 0$, in which case we take a shadow step.

Assuming oracle access to compute $d_x^{\Pi}(w)$ and $\hat{\lambda}_{i-1}$ for any $x \in \mathcal{P}$, Theorem 3 gives a constructive method for tracing the whole piecewise linear curve of $g_{x,w}(\cdot)$. We include this as an algorithm, $\text{TRACE}(x_0, x, w, \lambda_x)$, which traces the projections curve until a target step-size λ , and give its complete description in Algorithm 1. The following remarks about the TRACE algorithm (Algorithm 1) will be useful to understand its implementation and correctness:

Remark 1.

- (a) Theorem 3 applied for $i = 1$ implies that the first segment of the projections curve is given by walking maximally along the shadow, since:

$$\begin{aligned} \langle x_0 - \lambda_0^- \nabla h(x_0) - x_{i-1}, d_{x_{i-1}}^{\Pi}(\nabla h(x_0)) \rangle &= \langle x_0 - \lambda_0^- \nabla h(x_0) - x_0, d_{x_0}^{\Pi}(\nabla h(x_0)) \rangle \quad (i = 1) \\ &= \langle -\lambda_0^- \nabla h(x_0), d_{x_0}^{\Pi}(\nabla h(x_0)) \rangle \\ &= \langle 0, d_{x_0}^{\Pi}(\nabla h(x_0)) \rangle = 0, \end{aligned}$$

where we used the fact that $\lambda_0^- = 0$ by Lemma 1.

- (b) Whenever we take a shadow step in case (a), we are guaranteed to add a tight constraint at the subsequent breakpoint, since the next breakpoint is obtained by taking the maximum movement

[‡]The first order optimality condition for $\hat{d}_{x_{i-1}}^{\Pi}$ is $\langle -\nabla h(x_0) - \hat{d}_{x_{i-1}}^{\Pi}, y - \hat{d}_{x_{i-1}}^{\Pi} \rangle \leq 0$ for any feasible direction $y \in \text{Cone}(F - x_{i-1})$. Since $\langle -\nabla h(x_0) - \hat{d}_{x_{i-1}}^{\Pi}, \hat{d}_{x_{i-1}}^{\Pi} \rangle = 0$ by definition of $\hat{d}_{x_{i-1}}^{\Pi}$ and any $y \in \text{Cone}(F - x_{i-1})$ can be written as $\alpha(z - x_{i-1})$ for some $z \in F$ and $\alpha \geq 0$, this first order optimality condition reduces to $\langle -\nabla h(x_0) - \hat{d}_{x_{i-1}}^{\Pi}, z - x_{i-1} \rangle \leq 0 \forall z \in F$. Since $\langle d, -\nabla h(x_0) - d \rangle = 0$ and $\langle -\nabla h(x_0) - d, z - x_{i-1} \rangle \leq 0 \forall z \in F$, we have that d satisfies first-order optimality for $\hat{d}_{x_{i-1}}^{\Pi}$.

Algorithm 1 Tracing Parametric Projections Curve: $\text{TRACE}(x_0, x, w, \lambda_x)$

Input: Polytope $\mathcal{P} \subseteq \mathbb{R}^n$, starting point of the projections curve $x_0 \in \mathcal{P}$, $w \in \mathbb{R}^n$, and a point on the projections curve $x \in \mathcal{P}$ such that $g(\lambda_x) = \Pi_{\mathcal{P}}(x_0 - \lambda_x w) = x$, for a given λ_x .

Return: Next breakpoint y (if any) and step-size λ_y such that $g(\lambda_y) = y$.

- 1: Compute $d_x^{\Pi} := \lim_{\epsilon \downarrow 0} \frac{\Pi_{\mathcal{P}}(x - \epsilon w) - x}{\epsilon}$.
 - 2: **if** $d_x^{\Pi} \neq 0$ **then** ▷ check if we are at endpoint
 - 3: **if** $\langle x_0 - \lambda_x w - x, d_x^{\Pi} \rangle = 0$ **then** ▷ determine if we take shadow step
 - 4: Compute $\gamma^{\max} = \max\{\delta \mid x + \delta d_x^{\Pi} \in \mathcal{P}\}$ ▷ line-search in shadow direction
 - 5: Set $d = d_x^{\Pi}$. ▷ next linear direction we move in
 - 6: **else**
 - 7: $\hat{d}_x^{\Pi}, \gamma^{\max} = \text{TRACE-IN-FACE}(x_0, x, w, \lambda_x)$. ▷ in-face step
 - 8: Set $d = \hat{d}_x^{\Pi}$. ▷ next linear direction we move in
 - 9: **end if**
 - 10: Compute next break point $y = x + (\gamma^{\max})d$
 - 11: Update $\lambda_y^- = \lambda_x + \gamma^{\max}$. ▷ keep track of total step-size accrued
 - 12: **else** ▷ x is the endpoint of the curve
 - 13: Set $y = x$ and $\lambda_y = \lambda_x$ ▷ output does not change
 - 14: **end if**
- Return:** y, λ_y
-

Algorithm 2 Tracing in-face movement: $\text{TRACE-IN-FACE}(x_0, x, w, \lambda_x)$

Input: Polytope $\mathcal{P} \subseteq \mathbb{R}^n$, starting point of projections curve $x_0 \in \mathcal{P}$, current breakpoint $x \in \mathcal{P}$, direction $w \in \mathbb{R}^n$, and λ_x satisfying $g(\lambda_x) = \Pi_{\mathcal{P}}(x_0 - \lambda_x w) = x$.

- 1: Compute $\hat{d}_x^{\Pi} = (I - A_{I(x)}^{\dagger} A_{I(x)})(-w)$ ▷ in-face directional derivative at x
 - 2: Evaluate $\hat{\lambda} = \sup\{\lambda \mid N_{\mathcal{P}}(g(\lambda')) = N_{\mathcal{P}}(x_{i-1}) \forall \lambda' \in [\lambda_x, \lambda]\}$ ▷ see remark 3
- Return:** $\hat{d}_x^{\Pi}, \hat{\lambda}$
-

along the directional derivative $d_{x_{i-1}}^{\Pi}(\nabla h(x_0))$. However, this need not be true in case (b), unless the maximum in-face movement, i.e., $\hat{\lambda}_{i-1} = \lambda_{i-1}^+ + \max\{\delta : x_{i-1} + \delta \hat{d}_{x_{i-1}}^{\Pi}(\nabla h(x_0)) \in \mathcal{P}\}$.

(c) We can directly prove Theorem 2 (a)-(b) (i)-(iii) using this theorem and induction.

(d) Note that whenever we take an in-face step we have that $\hat{d}_{x_{i-1}}^{\Pi}(\nabla h(x_0)) \neq d_{x_{i-1}}^{\Pi}(\nabla h(x_0))$. This is because we take an in-face step whenever $\langle p_{i-1}, d_{x_{i-1}}^{\Pi}(\nabla h(x_0)) \rangle \neq 0$; however, $\langle p_{i-1}, \hat{d}_{x_{i-1}}^{\Pi}(\nabla h(x_0)) \rangle = 0$ always since p_{i-1} is in the rowspace of $A_{(x_i)}$ and $\hat{d}_{x_{i-1}}^{\Pi}(\nabla h(x_0))$ is in the null-space of $A_{(x_i)}$ by definition.

(e) If $\lambda_{i-1} < \lambda_{i-1}^+$, then projections curve moves trivially in-face in the interval $[\lambda_{i-1}, \lambda_{i-1}^+]$ with $\hat{d}_{x_{i-1}}^{\Pi}(\nabla h(x_0)) = 0$ where we obtain $\lambda_{i-1}^+ = \hat{\lambda}_{i-1}$; otherwise, we walk in-face along $\hat{d}_{x_{i-1}}^{\Pi}(\nabla h(x_0)) \neq 0$ until $\lambda_i^- := \hat{\lambda}_{i-1}$.

Remark 2. Computing maximum in-face movement. Suppose that we are at a breakpoint x and we have that $\langle x_0 - \lambda_x w - x, d_x^{\Pi} \rangle \neq 0$. Computing $\hat{\lambda}$ amounts to finding the maximum λ such

that $x_0 - \lambda w - (x + (\lambda - \lambda_x)\hat{d}_x^\Pi) \in N_{\mathcal{P}}(x + (\lambda - \lambda_x)\hat{d}_x^\Pi)$ and $x + (\lambda - \lambda_x)\hat{d}_x^\Pi \in \mathcal{P}$, which can be computed by the solving the following linear program:

$$\begin{aligned}
& \max \lambda \\
& \text{s.t. } x_0 - \lambda w - x - (\lambda - \lambda_x)\hat{d}_x^\Pi = A_{I(x)}^\top \mu, \\
& \quad x + (\lambda - \lambda_x)\hat{d}_x^\Pi \in \mathcal{P}, \\
& \quad \mu \geq 0.
\end{aligned} \tag{12}$$

Note that $\lambda = \lambda_x$ is a feasible solution to (12), which is also the optimal solution when the projections curve is moving to another facet and not moving in-face (case (b) in Theorem 3). Furthermore, it is easy to see that (12) is bounded, and thus always has an optimal solution. Though it is an open question to bound the number of breakpoints for any general polytope, we show a simple bound next which depends on the number of faces of the polytope:

Theorem 4 (Bound on breakpoints in parametric projections curve). *Let $\mathcal{P} \subseteq \mathbb{R}^n$ be a polytope with m facet inequalities (e.g., as in (3)). Then, the total number of breakpoints of the projections curve is $O(2^m)$ steps.*

Proof. Note that once the projections curve leaves the interior of a face, it can no longer visit that face again, since the equivalence of normal cones at two projections implies the projections curve is linear between the two points (which must necessarily lie on the same face) (Theorem 2 (v)). Thus, the number of breakpoints can be at most the number of faces, i.e., $O(2^m)$. \square

Although the previous theorem establishes a worst-case exponential bound on the number of breakpoints of the projections curve, we next prove that the number of breakpoints of the projections curve is at most n (the dimension) for both the simplex and the hypercube. Later, this distinction will be important when we benchmark our algorithm against the Away-steps Frank-Wolfe (AFW) variant of Lacoste-Julien and Jaggi [10]. Recall, the convergence rate of AFW depends on the pyramidal-width of the polytope. To the best of our knowledge, the pyramidal-width has only been evaluated on the hypercube ($\rho = \frac{1}{\sqrt{n}}$ for the hypercube) and probability simplex ($\rho = \frac{2}{\sqrt{n}}$ for the simplex), due to its complexity [10]. Using our next results, we will show that we obtain an $\Omega(n^2)$ factor reduction in convergence rates and iteration complexity compared to AFW. We remark that our following results might be of independent interest to the discrete-geometry community.

Theorem 5 (Breakpoints for the Hypercube). *Consider the n -dimensional hypercube $\mathcal{H}_n := \{x \in \mathbb{R}^n \mid 0 \leq x_i \leq 1 \forall i \in [n]\}$ and fix $x_0 \in \mathcal{H}_n$. Then, the projections curve $g(\lambda) = \Pi_{\mathcal{P}}(x_0 - \lambda w)$ has only $O(n)$ breakpoints (for $\lambda \geq 0$).*

The proof of this theorem follows by simply tracking first-order optimality conditions to show

Algorithm 3 Shadow over Simplex: SHADOW-SIMPLEX(x, w)

Input: Point $x \in \Delta_n$ and direction $w \in \mathbb{R}^n$.

- 1: Set $g = -w$ and define $I = \{i \in [n] \mid x_i = 0\}$
- 2: Let $[u_x]_i = 0$ if $i \in I$ and $[u_x]_i = 1$ otherwise. \triangleright support of x
- 3: Compute $d = g \odot u_x - \langle g, u_x \rangle u_x / \|u_x\|^2$ \triangleright project g onto hyperplane $\mathbb{1}^\top u_x = 0$
- 4: Let \tilde{I} be an ordering of I such that $g_{\tilde{I}_1} \geq \dots \geq g_{\tilde{I}_{|I|}}$. $\triangleright \tilde{I} = \text{sort}(i \in I, \text{key} = g[i])$
- 5: **for** $i \in \tilde{I}$ **do**
- 6: Set $u_x' = u_x$ and $u_{x_i}' = 1$
- 7: Compute $d' = g \odot u_x' - \langle g, u_x' \rangle u_x' / \|u_x'\|^2$ \triangleright project g onto hyperplane $\mathbb{1}^\top u_x' = 0$
- 8: **If** $d'_i \geq 0$ for all $i \in I$, then set $d = d'$ and $u_x = u_x'$
- 9: **Else break**
- 10: **end for**

Return: d

that the shadow direction $d_x^\Pi(w)$ is given by

$$[d_x^\Pi(w)]_i = \begin{cases} 0 & \text{if } i \in I_1 \text{ and } [-w]_i \leq 0; \\ 0 & \text{if } i \in I_2 \text{ and } [-w]_i \geq 0; \\ [-w]_i & \text{otherwise.} \end{cases} \quad (13)$$

where $I_1 := \{i \in [n] \mid x_i = 0\}$ and $I_2 := \{i \in [n] \mid x_i = 1\}$ denote the index sets of tight constraints at x .

Interestingly, we can further show that there are no in-face steps in the projection curve, and therefore, the number of breakpoints is at most n (proof in Appendix C.1). Due to the structure of the shadow (equation (13)), it can be computed in $O(n)$ time, and the entire projections curve can be computed in $O(n^2)$ time.

Similarly, we can show that the number of breakpoints in the projections curve over the simplex is also $O(n)$:

Theorem 6 (Breakpoints for the Simplex). *Let $\Delta_n := \{x \in \mathbb{R}^n \mid \sum_{i=1}^n x_i = 1, x_i \geq 0 \forall i \in [n]\}$ denote the $(n - 1)$ -dimensional simplex and fix $x_0 \in \Delta_n$. Then, the projections curve $g(\lambda) = \Pi_P(x_0 - \lambda w)$ has only $O(n)$ breakpoints (for $\lambda \geq 0$).*

To prove this theorem, similar to the hypercube, we first characterize the shadow direction over the simplex and include a new algorithm to compute the shadow in $O(n^2 + n \log n)$ time:

Lemma 4. *Consider any $x \in \Delta_n$ and any direction $w \in \mathbb{R}^n$, Then, the output of SHADOW-SIMPLEX(x, w) (Algorithm 3) is $d_x^\Pi(w)$. Moreover, the running time of the algorithm is $O(n \log n + n^2)$ time.*

The idea of the proof is as follows; see Appendix C.2 for a full proof. Recall that $d_x^\Pi(w) = \arg \min_{d \in T_{\Delta_n}(x)} \|-w - d\|^2$, where $T_{\Delta_n}(x)$ is the tangent cone for the simplex at x . Letting, $I := \{i \in [n] \mid x_i = 0\}$ be the index-set of tight constraints at x , we can re-write this optimization problem as $d_x^\Pi(w) = \arg \min_{d \in \mathbb{R}^n} \{\|-w - d\| \mid \sum_{i=1}^n d_i = 0, d_i \geq 0 \forall i \in I\}$. Furthermore, letting

$I^* = \{i \in I \mid d_x^\Pi(w)_i = 0\}$ be the index-set of coordinates where the shadow $d_x^\Pi(w)_i = 0$, we can write $d_x^\Pi(w) = \arg \min_{d \in \mathbb{R}^n} \{\|g - d\|^2 \mid \sum_{i=1}^n d_i = 0, d_i = 0 \text{ for all } i \in I^*\}$, which can be computed in closed form using $d := -w \odot r - \frac{\langle -w, r \rangle}{\|r\|^2} r = d_x^\Pi(w)^{**}$ where $r \in \mathbb{R}^n$ is the vector defined by $r_i = 0$ if $i \in I^*$ and $r_i = 1$ otherwise. Using optimality conditions over the simplex, we show that the support of I^* coincides with the smallest values of $-w$. In the algorithm, we exploit this property and sort w in $O(n \log n)$ time, and then search for I^* within I greedily, which takes $O(n^2)$ time.

Next, to prove Theorem 6, we show that there are again no in-face steps in the projections curve over the simplex, and we have n consecutive maximal shadow steps until the end point of the curve is reached. In each maximal shadow step, using the structure of the shadow given by the previous lemma, we show that we zero out a coordinate in x_0 until we reach the endpoint of the projections curve, which is a vertex of the simplex. This takes at most $n - 1$ maximal shadow steps, i.e. the number of breakpoints of the projections curve $\beta \leq n$ (proof in Appendix C.3). Thus, we can compute the entire projections curve in $O(n^3)$ time.

4 Descent Directions

Having characterized the properties of the parametric projections curve, we highlight connections between descent directions in conditional gradient and projected gradient methods. We first highlight a connection between the shadow and the *gradient mapping*. Given any scalar $\eta > 0$, the gradient mapping is defined as $G_\eta(x) := \eta(x - \Pi_{\mathcal{P}}(x - \nabla h(x)/\eta)) = \eta(x - g(1/\eta))$ ^{††}. The typical update in gradient mapping is $x_{t+1} = x_t - \frac{1}{\eta} G_\eta(x_t)$, which corresponds to a single projection step under the Euclidean norm. Some recent variants of gradient mapping [31] explore more elaborate update steps (using varying step-sizes in the same direction $G_\eta(x)$), however, these movements are interior to the polytope (typically), and thus very different from SHADOW-WALK.

We next claim that the shadow is the best local feasible direction of descent in the following sense: it has the highest inner product with the negative gradient compared to any other normalized feasible direction. In other words, it is the analog of the negative gradient for constrained optimization.

Lemma 5 (Steepest feasible descent of Shadow Steps). *Let $\mathcal{P} \subseteq \mathbb{R}^n$ be a polytope defined as in (3) and let $x \in \mathcal{P}$ with gradient $\nabla h(x)$ be given. Let y be any feasible direction at x , i.e., $\exists \gamma > 0$ s.t. $x + \gamma y \in \mathcal{P}$. Then*

$$\left\langle -\nabla h(x), \frac{d_x^\Pi}{\|d_x^\Pi\|} \right\rangle^2 = \|d_x^\Pi\|^2 \geq \left\langle d_x^\Pi, \frac{y}{\|y\|} \right\rangle^2 \geq \left\langle -\nabla h(x), \frac{y}{\|y\|} \right\rangle^2. \quad (14)$$

This result is intuitive as d_x^Π is the projection of $-\nabla h(x)$ onto the set of feasible directions at x ; this is the fact crucially used to prove this result (proof in Appendix D.1). The above lemma will be useful in the convergence proof for our novel SHADOW-CG (Theorem 11) and SHADOW-CG² (Theorem 12) algorithms. We also show that the shadow gives a true estimate of convergence to

**We use \odot to denote a Hadamard product operation.

††Note that $g(1/\eta)$ can be obtained using $\text{TRACE}(x, \nabla h(x), 1/\eta, 0)$.

optimal, in the sense that $\|d_x^\Pi\| = 0$ if and only if $x = \arg \min_{x \in \mathcal{P}} h(x)$ (Lemma 6). On the other hand, note that $\|\nabla h(x)\|$ does not satisfy this property and can be strictly positive at the constrained optimal solution. Moreover, applying the Cauchy-Schwarz inequality to the left hand side of (14), for any $x \in \mathcal{P}$, we have

$$\|\nabla h(x)\|^2 \geq \|d_x^\Pi\|^2, \quad (15)$$

and so we have a tighter primal gap bound. In addition, for μ -strongly convex functions, we show that $\|d_x^\Pi\|^2 \geq 2\mu(h(x) - h(x^*))$. Hence, $\|d_{x^{(t)}}^\Pi\|$ is a natural quantity for estimating primal gaps without any dependence on geometric constants like those used in other CG variants such as AFW.

Lemma 6 (Primal gap estimate). *Let $\mathcal{P} \subseteq \mathbb{R}^n$ be a polytope and fix any $x \in \mathcal{P}$. Consider any convex function $h : \mathcal{P} \rightarrow \mathbb{R}$ and let $x^* \in \arg \min_{x \in \mathcal{P}} h(x)$. Then, $\|d_x^\Pi\| = 0$ if and only if $x = x^*$, where $x^* = \arg \min_{x \in \mathcal{P}} h(x)$. Moreover, if h is μ -strongly convex over \mathcal{P} , then*

$$\|d_x^\Pi\|^2 \geq 2\mu(h(x) - h(x^*)). \quad (16)$$

The proof follows from first-order optimality and can be found in Appendix D.2. The above lemma is a generalization of the PL-inequality [26], which states that $\|\nabla h(x)\|^2 \geq 2\mu(h(x) - h(x^*))$ when h is μ -strongly convex. Note that we bound the primal-gap in terms of the norm of the shadow in (16), instead of the gradient in PL-inequality. This is also a stronger condition compared to the analogous one which involves bounding with respect to the Frank-Wolfe gap.

We next show that the end point of the projections curve is in fact the FW vertex under mild technical conditions. In other words, FW vertices are the projection of an infinite descent in the direction of the negative gradient (Theorem 7). Thus, FW vertices are able to obtain the maximum movement in the negative gradient direction while remaining feasible compared to PGD, thereby giving FW-steps a new perspective.

Theorem 7 (Optimism of FW vertex). *Let $\mathcal{P} \subseteq \mathbb{R}^n$ be a polytope and let $x \in \mathcal{P}$. Let $g(\lambda) = \Pi_{\mathcal{P}}(x - \lambda \nabla h(x))$ for $\lambda \geq 0$. Then, the end point of this curve is: $\lim_{\lambda \rightarrow \infty} g(\lambda) = v^* = \arg \min_{v \in F} \|x - v\|^2$, where $F = \arg \min_{v \in \mathcal{P}} \langle \nabla h(x), v \rangle$ is the face of \mathcal{P} that minimizes the gradient $\nabla h(x)$. In particular, if F is a vertex, then $\lim_{\lambda \rightarrow \infty} g(\lambda) = v^*$ is the FW vertex.*

Proof. If $\nabla h(x) = 0$, then $g(\lambda) = x$ for all $\lambda \in \mathbb{R}^n$, and the theorem holds trivially, so assume otherwise. Let $x_i \in \mathcal{P}$ be the i th breakpoint in the projections curve $g(\lambda) = \Pi_{\mathcal{P}}(x_0 - \lambda \nabla h(x_0))$, with $x_i = x$ for $i = 0$. Using Theorem 4, we know that the number of breakpoints curve $k \leq 2^m$. Consider the last breakpoint x_k in the curve and let $\lambda_k^- = \min\{\lambda \geq 0 \mid g(\lambda) = x_k\}$. We will now show that $x_k = v^*$.

- (i) We first show that $x_k \in F$, i.e. $-\nabla h(x) \in N_{\mathcal{P}}(x_k)$. Suppose for a contradiction that this not true. Then there exists some $z \in \mathcal{P}$ such that $\langle -\nabla h(x), z - x_k \rangle > 0$. Consider any scalar $\bar{\lambda}$ satisfying $\bar{\lambda} > \max\{-\frac{\langle x - x_k, z - x_k \rangle}{\langle -\nabla h(x), z - x_k \rangle}, \lambda_k^-\}$. Then, using the choice of $\bar{\lambda}$ we have

$$\langle x - x_k, z - x_k \rangle + \bar{\lambda} \langle -\nabla h(x), z - x_k \rangle > 0 \implies \langle x - x_k - \bar{\lambda} \nabla h(x), z - x_k \rangle > 0.$$

Now, since $g(\lambda) = x_k$ for $\lambda \geq \lambda_k^-$, we have $g(\bar{\lambda}) = x_k$. Thus, the above equation could be written as $\langle x - \bar{\lambda} \nabla h(x) - g(\bar{\lambda}), z - g(\bar{\lambda}) \rangle > 0$, which contradicts the first-order optimality for $g(\bar{\lambda})$.

- (ii) We will now show that x_k is additionally the closest point to x in ℓ_2 norm. Again, suppose for contradiction that this not true. Let $\epsilon := \|x_k - v^*\| > 0$. First, note that by definition, $g(\lambda) = \arg \min_{y \in \mathcal{P}} \left\{ \frac{\|x-y\|^2}{2\lambda} + \langle \nabla h(x), y \rangle \right\}$ for any $\lambda > 0$. Then, since $g(\lambda_k^-) = x_k$ we have

$$\frac{\|x - x_k\|^2}{2\lambda_k^-} + \langle \nabla h(x), x_k \rangle \leq \frac{\|x - z\|^2}{2\lambda_k^-} + \langle \nabla h(x), z \rangle, \quad \forall z \in \mathcal{P}. \quad (17)$$

The first-order optimality condition for v^* (for minimizing $\|x - y\|^2$ over $y \in F$) implies $\langle v^* - x, z - v^* \rangle \geq 0$ for all $z \in F$. In particular, $(v^* - x)^\top (x_k - v^*) \geq 0$ since $x_k \in F$. Therefore,

$$\|x - v^*\|^2 + \|x_k - v^*\|^2 = \|x\|^2 + 2\|v^*\|^2 - 2x^\top v^* + \|x_k\|^2 - 2x_k^\top v^* \quad (18)$$

$$= \|x_k - x\|^2 - 2(v^* - x)^\top (x_k - v^*) \quad (19)$$

$$\leq \|x_k - x\|^2. \quad (20)$$

But then, since $x_k \in F$, we know that $\langle \nabla h(x), x_k \rangle = \langle \nabla h(x), v^* \rangle$, which implies

$$\begin{aligned} \frac{\|x - v^*\|^2}{2\lambda_k^-} + \langle \nabla h(x), v^* \rangle &\leq \frac{\|x_k - x\|^2 - \|x_k - v^*\|^2}{2\lambda_k^-} + \langle \nabla h(x), v^* \rangle && \text{(using (20))} \\ &= \frac{\|x_k - x\|^2 - \epsilon}{2\lambda_k^-} + \langle \nabla h(x), v^* \rangle && (\|x_k - v^*\| = \epsilon) \\ &< \frac{\|x_k - x\|^2}{2\lambda_k^-} + \langle \nabla h(x), x_k \rangle, && (\epsilon > 0) \end{aligned}$$

contradicting the optimality of x_k (17).

□

Next, we show that the shadow steps also give the best away direction emanating from away-vertices in the minimal face at any $x \in \mathcal{P}$ (which is precisely the set of *possible* away vertices (see Lemma 10 in [32]), using Lemma 5 and the following result (the proof in Appendix D.3):

Lemma 7 (Away-steps). *Let $\mathcal{P} \subseteq \mathbb{R}^n$ be a polytope defined as in (3) and fix $x \in \mathcal{P}$. Let $F = \{z \in \mathcal{P} : A_{I(x)} z = b_{I(x)}\}$ be the minimal face containing x . Further, choose $\delta_{\max} = \max\{\delta : x - \delta d_x^\Pi \in \mathcal{P}\}$ and consider the away point $a_x = x - \delta_{\max} d_x^\Pi$ obtained by moving maximally along the the direction of the negative shadow. Then, a_x lies in F and the corresponding away-direction is simply $x - a_x = \delta_{\max} d_x^\Pi$.*

Lemma 7 states that the away point obtained by the maximal movement along the negative shadow from x , a_x , lies in the convex hull of $A := \{v \in \text{vert}(P) \cap F\}$. The set A is precisely the set

of all possible away vertices (see Lemma 10 in [32]). Thus, the shadow gives the best direction of descent emanating from the convex hull of all possible away-vertices.

5 Continuous-time Dynamics and SHADOW-WALK Algorithm

Consider an iterative descent method for solving $\min_{x \in \mathbb{R}^n} h(x)$ and let $x^{(t)}$ be an iterate of this method. If we were to take an ϵ step in any direction from $x^{(t)}$ to minimize h , then we would move along the negative gradient, i.e., $x^{(t)} - \epsilon \nabla h(x^{(t)})$, since it results in the highest local progress as the negative gradient is the direction of steepest descent in unconstrained optimization. Furthermore, it is known that the algorithm obtained by walking along the negative gradient, i.e. gradient descent, has linear convergence for smooth and strongly convex functions in unconstrained optimization [33]. However, the negative gradient may no longer be feasible for constrained optimization. We established in the last section that the shadow of the negative gradient $d_{x^{(t)}}^{\Pi}$ is indeed the best “local” direction of descent (Lemma 5), i.e. it is steepest descent direction for constrained optimization and is a true measure of the primal gap since convergence in $\|d_{x^{(t)}}^{\Pi}\|$ implies optimality (Lemma 6). Having characterized the parametric projections curve, the natural question is if a shadow-descent algorithm that walks along the directional derivative with respect to the negative gradient at iterate $x^{(t)}$, converges linearly. We start by answering that question positively in continuous-time.

We present the continuous-time dynamics for moving along the shadow of the gradient in the polytope \mathcal{P} . To do that, we briefly review the Mirror Descent (MD) algorithm; our exposition uses the mirror-map view of MD proved by Beck and Teboulle in 2003 [34]. The MD algorithm is defined with the help of a strongly-convex and differentiable function $\phi : \mathcal{P} \rightarrow \mathbb{R}$, known as a distance-generating function. The Fenchel Conjugate of ϕ is defined by $\phi^*(y) = \max_{x \in \mathcal{P}} \{\langle x, y \rangle - \phi(x)\}$. From Danskin’s theorem (see e.g., [35]), we know that $\nabla \phi^*(y) = \arg \max_{x \in \mathcal{P}} \{\langle y, x \rangle - \phi(x)\}$. The mirror descent algorithm is iterative and starts with a point $x^{(0)} \in \mathcal{P}$. Then, for any $t \geq 1$, the algorithm first performs *unconstrained* gradient descent steps in the dual space using $\nabla \phi$ (in our case since $\mathcal{P} \subseteq \mathbb{R}^n$, the dual space is identified with \mathbb{R}^n):

$$z^{(t)} = \nabla \phi(x^{(t)}) - \gamma_t \nabla h(x^{(t)}) \text{ for some step size } \gamma_t \geq 0,$$

and then maps back these descent steps to the primal space by computing a so-called *Bregman projection*, which under the mirror-map view could be computed as follows : $x^{(t+1)} = \nabla \phi^*(z^{(t)})$.

5.1 ODE for Moving in the Shadow of the Gradient

Let $X(t)$ denote the continuous-time trajectory of our dynamics and \dot{X} denote the time-derivative of $X(t)$, i.e., $\dot{X}(t) = \frac{d}{dt} X(t)$. In [36], Krichene et. al propose the following coupled dynamics $(X(t), Z(t))$ for mirror descent, where $X(t)$ evolves in the primal space (i.e. domain of $\nabla \phi$), and $Z(t)$ evolves in the dual space (i.e. domain of $\nabla \phi^*$) as follows, initialized with $Z(0) = z^{(0)} \in$

$\text{dom}(\nabla\phi^*)$ with $\nabla\phi^*(z^{(0)}) = x^{(0)} \in \mathcal{P}$:

$$\dot{Z}(t) = -\nabla h(X(t)), \quad X(t) = \nabla\phi^*(Z(t)). \quad (21)$$

Let $d_{X(t)}^\phi$ be the directional derivative with respect to the Bregman projections in the mirror descent algorithm, i.e., $d_{X(t)}^\phi = \lim_{\epsilon \downarrow 0} \frac{\nabla\phi^*(\nabla\phi(X(t)) - \epsilon\nabla h(X(t))) - X(t)}{\epsilon}$. The continuous time dynamics of tracing this directional derivative are simply

$$\dot{X}(t) = d_{X(t)}^\phi. \quad (22)$$

These dynamics in (22) solely operate in the primal space and one can initialize them with $X(0) = x^{(0)} \in \mathcal{P}$ and show that they are equivalent to (21) under mild conditions (proof in Appendix E.1):

Theorem 8. *Assume that the directional derivative $d_{X(t)}^\phi$ exists for all $t \geq 0$. Then, the dynamics for mirror descent (21) are equivalent to the shadow dynamics $\dot{X}(t) = d_{X(t)}^\phi$ with the same initial conditions $X(0) = x^{(0)} \in \mathcal{P}$.*

Although the results of Theorem 8 hold for general mirror-maps, in this work we focus on the case when $\phi = \frac{1}{2}\|\cdot\|^2$, in which case $d_{X(t)}^\phi = d_{X(t)}^\Pi$ to exploit the piecewise linear structure of the projections curve. Therefore, Theorem 8 shows that the continuous-time dynamics of moving in the (Euclidean) shadow of the gradient are equivalent to those of PGD. Moreover, we also show the following convergence result of those dynamics (the proof is in Appendix E.2):

Theorem 9. *Let $\mathcal{P} \subseteq \mathbb{R}^n$ be a polytope and suppose that $h : \mathcal{P} \rightarrow \mathbb{R}$ is differentiable and μ -strongly convex over \mathcal{P} . Consider the shadow dynamics $\dot{X}(t) = d_{X(t)}^\Pi$ with initial conditions $X(0) = x^{(0)} \in \mathcal{P}$. Then for each $t \geq 0$, we have $X(t) \in \mathcal{P}$. Moreover, the primal gap associated with the shadow dynamics decreases as:*

$$h(X(t)) - h(x^*) \leq e^{-2\mu t} h(X(0)) - h(x^*).$$

5.2 Shadow-Walk Method

Although the continuous-dynamics of moving along the shadow are the same as those of PGD and achieve linear convergence, it is unclear how to discretize this continuous-time process and obtain a linearly convergent algorithm. To ensure feasibility we may have arbitrarily small step-sizes, and therefore, cannot show sufficient progress in such cases. This issue occurs in existing FW variants that use some form of away-steps. In fact, many recent papers [10, 3, 37, 38, 20, 19, 39, 16, 40, 41] use a similar way of showing convergence by bounding the number of such ‘bad’ steps with dimension reduction arguments, which crucially rely on maintaining iterates as a convex combination of vertices. However, unlike away-steps in CG variants, we consider shadow directions (d_x^Π, \hat{d}_x^Π) for constrained descent that enable us to give a novel geometry-independent proof of convergence. This method, SHADOW-WALK, effectively mimics a projected gradient descent algorithm^{‡‡}, except it uses the

^{‡‡}Gradient mapping is equivalent under Euclidean prox operator is equivalent to projected gradient descent, however the direction of movement is in the interior of the polytope (for large enough step sizes), whereas SHADOW-WALK moves on the boundary of the polytope, which will be a crucial difference in the discretization.

Algorithm 4 SHADOW-WALK Algorithm

Input: Polytope $\mathcal{P} \subseteq \mathbb{R}^n$, function $h : \mathcal{P} \rightarrow \mathbb{R}$ and initialization $x^{(0)} \in \mathcal{P}$.

1: **for** $t = 0, \dots, T$ **do**

2: Update $x^{(t+1)} := \text{TRACE-OPT}(x^{(t)}, \nabla h(x^{(t)}))$. ▷ trace projections curve

3: **end for**

Return: $x^{(T+1)}$

projections curve to reach the desired unconstrained descent. Although simple, this will help us interpolate between constrained descent optimization methods and projected gradient descent, and achieve an affine-invariant rate for SHADOW-CG.

We propose SHADOW-WALK (Algorithm 4): to trace the projections curve by walking along the shadow at an iterate $x^{(t)}$ until enough progress is ensured. In general, note that the shadow ODE might revisit a fixed facet a large number of times (see Figure 1) with decreasing step-sizes; and the step-size along which one can move along shadow might be arbitrarily small to ensure feasibility, in which case we cannot show a sufficient decrease in primal gap to prove a global convergence rate. To solve these two issues, we borrow the notion of “enough progress” from PGD, and trace the projections curve until effectively a stepsize of $1/L$ is achieved in unconstrained descent (where L is the smoothness constant). We use the TRACE-OPT procedure to do this, which chains together consecutive short descent steps and uses line-search until it minimizes the function h over the linear segments of projections curve. The complete description of the algorithm is given in Algorithm 7 in Appendix A. This process remedies the aforementioned issue of diminishing step-sizes and enables us to prove a global linear convergence rate^{§§}.

Each TRACE-OPT call only requires one gradient oracle call. This results in linear convergence, as long as the number of steps taken by the TRACE-OPT procedure are bounded, i.e., the number of “bad” boundary cases. This is at most the number of breakpoints in the projections curve, which we show linear bounds for the simplex and hypercube (Theorems 5, 6), but this could be large in general (Theorem 4). We thus establish the following result (proof in Appendix E.3):

Theorem 10. *Let $\mathcal{P} \subseteq \mathbb{R}^n$ be a polytope and suppose that $h : \mathcal{P} \rightarrow \mathbb{R}$ is L -smooth and μ -strongly convex over \mathcal{P} . Then the primal gap of the SHADOW-WALK algorithm decreases geometrically:*

$$(h(x^{(t+1)}) - h(x^*)) \leq \left(1 - \frac{\mu}{L}\right) (h(x^{(t)}) - h(x^*))$$

with each iteration of the SHADOW-WALK algorithm (assuming TRACE-OPT is a single step). Moreover, the number of oracle calls to shadow, in-face shadow and line-search oracles to obtain an ϵ -accurate solution is $O\left(\beta \frac{L}{\mu} \log\left(\frac{1}{\epsilon}\right)\right)$, where β is the maximum number of breakpoints of the parametric projections curve that the TRACE-OPT method visits.

Comparing the convergence rate of SHADOW-WALK with rate of the ODE in Theorem 9, we see

^{§§}Tapia et al. [28] prove that the limit point of the sequence of iterates obtained by walking along the shadow (with appropriately chosen step sizes to ensure feasibility) converges to a stationary point. However, they did not give global convergence rates.

Algorithm 5 Shadow Conditional Gradient (SHADOW-CG)

Input: Polytope $\mathcal{P} \subseteq \mathbb{R}^n$, function $f : P \rightarrow \mathbb{R}$, $x_0 \in P$ and accuracy parameter ε .

- 1: **for** $t = 0, \dots, T$ **do**
- 2: Let $v^{(t)} := \arg \min_{v \in P} \langle \nabla h(x^{(t)}), v \rangle$ and $d_t^{\text{FW}} := v^{(t)} - x^{(t)}$. ▷ FW direction
- 3: **if** $\langle -\nabla h(x^{(t)}), d_t^{\text{FW}} \rangle \leq \varepsilon$ **then return** $x^{(t)}$ ▷ primal gap is small enough
- 4: Compute the derivative of projection of the gradient $d_{x^{(t)}}^{\Pi}$
- 5: **if** $\langle -\nabla h(x^{(t)}), d_{x^{(t)}}^{\Pi} / \|d_{x^{(t)}}^{\Pi}\| \rangle \leq \langle -\nabla h(x^{(t)}), d_t^{\text{FW}} \rangle$
- 6: $d_t := d_t^{\text{FW}}$ and $x^{(t+1)} := x^{(t)} + \gamma_t d_t$ ($\gamma_t \in [0, 1]$). ▷ use line-search
- 7: **else** $x^{(t+1)} := \text{TRACE-OPT}(x^{(t)}, \nabla h(x^{(t)}))$. ▷ trace projections curve
- 8: **end for**

Return: $x^{(t+1)}$

that we pay for its discretization with the constants L and β . Although our linear convergence rate depends on the number of facet inequalities m , it eliminates affine-variant constants needed in CG variants. For example, Jaggi and Lacoste-Julien [10] prove a contraction of $\left(1 - \frac{\mu}{L} \left(\frac{\rho}{D}\right)^2\right)$ in the objective to get an ε -approximate solution for the away-step FW algorithm, where ρ is the pyramidal-width of the domain. Although FW is known to be an affine-invariant algorithm, the pyramidal width is affine-variant (e.g., see Figure 3 for an example), whereas the number of breakpoints β does not increase with affine transformations. Moreover, unlike β , the pyramidal-width has no known worst-case lower bounds for general polytopes.

6 Shadow Conditional Gradient Method

We have shown so far that shadow steps are “best” away-steps (Lemma 7), and SHADOW-WALK is the constrained descent analogue of projected gradient descent. We also have seen that Frank-Wolfe vertices are the maximal movements one can obtain using a projected gradient descent step from any point (Theorem 7). We next propose a new method SHADOW-CG which uses Frank-Wolfe steps earlier in the algorithm and shadow steps more frequently towards the end of the algorithm to achieve the best-of-both-worlds. Frank-Wolfe steps allow us skip tracing a lot of breakpoints in the projections curve earlier in the optimization, and shadow steps reduce zig-zagging close to the optimal solution. To obtain a computable proxy for when to switch, we note that Frank-Wolfe directions become close to orthogonal to the negative gradient towards the end of the algorithm. However, in this case the norm of the shadow also starts diminishing (Lemma 6). Therefore, we propose to choose the FW direction in line 7 of Algorithm 5 whenever $\langle -\nabla h(x^{(t)}), d_t^{\text{FW}} \rangle \geq \langle -\nabla h(x^{(t)}), d_{x^{(t)}}^{\Pi} / \|d_{x^{(t)}}^{\Pi}\| \rangle = \|d_{x^{(t)}}^{\Pi}\|$, and shadow directions otherwise. This is sufficient to give provable linear convergence.

Theorem 11. *Let $\mathcal{P} \subseteq \mathbb{R}^n$ be a polytope with diameter D and suppose that $f : P \rightarrow \mathbb{R}$ is L -smooth and μ -strongly convex over P . Then, the primal gap $h(x^{(t)}) := h(x^{(t)}) - h(x^*)$ of SHADOW-CG decreases geometrically:*

$$h(x^{(t+1)}) \leq \left(1 - \min \left\{ \frac{1}{2}, \frac{\mu}{LD^2}, \frac{\mu}{L} \right\}\right) h(x^{(t)}),$$

with each iteration of the SHADOW-CG algorithm (assuming TRACE-OPT is a single step). Moreover, the running time to compute an ϵ -approximate solution is $O\left((D^2 L_O + \beta S) \frac{L}{\mu} \log\left(\frac{1}{\epsilon}\right)\right)$, where β is the number of breakpoints of the parametric projections curve that the TRACE-OPT method visits, S is the number of calls to the shadow oracle (or in-face), and L_O is the time for linear optimization.

Before we get into the proof of this worst-case running time, we want to highlight a few implications. Note that we remove the dependence of the running time on the pyramidal width. This implies that the running time is now affine-invariant, since β does not increase with affine transformations. For example, for a scaled simplex, $\sum_{e \neq e'} x_e + M x_{e'} \leq 1$, $x_e \geq 0$, $M \gg 1$, as M increases, the pyramidal width goes to zero, making the AFW running time prohibitely large, whereas the number of breakpoints remains $O(n)$. Second, since Frank-Wolfe steps skip a lot of projections, the number of projections required is much less than the worst-case in the above bound, as can be seen in our computations. Therefore, SHADOW-CG enjoys the best of both worlds. We now prove the theorem:

Proof. In the algorithm, we either enter the TRACE-OPT procedure (in which case we have $x^{(t+1)} := \text{TRACE-OPT}(x^{(t)}, \nabla h(x^{(t)}))$), or we take a Frank-Wolfe step ($x^{(t+1)} := x^{(t)} + \gamma_t(v^{(t)} - x^{(t)})$) for some $\gamma_t \in [0, 1]$. We split the proof of convergence into two cases depending on which case happens:

Case 1: *We enter the TRACE-OPT procedure.* Since $x^{(t+1)} := \text{TRACE}(x^{(t)}, \nabla h(x^{(t)}))$ and $\text{TRACE}(x^{(t)}, \nabla h(x^{(t)}))$ traces the whole curve of $g(\lambda) = \Pi_P(x^{(t)} - \lambda \nabla h(x^{(t)}))$ until we hit the $1/L$ step size with exact line-search, it follows that $h(x^{(t+1)}) \leq h(g(1/L))$, and we are thus guaranteed to make at least as much progress per iteration as that of projected gradient descent (PGD) step with a fixed-step size of $1/L$. Hence we get the same standard rate $(1 - \frac{L}{L})$ of decrease as PGD with fixed step size $1/L$ [33].

Case 2: *We take a Frank-Wolfe step.* Let γ_t be the step size chosen by line-search for moving along the chosen FW direction $d_t := v^{(t)} - x^{(t)}$, and let $\gamma_t^{\max} = 1$ be the maximum step-size that one can move along d_t . Using the smoothness of f , we have $h(x^{(t+1)}) \leq h(x^{(t)}) + \gamma_t \langle \nabla h(x^{(t)}), d_t \rangle + \frac{L \gamma_t^2}{2} \|d_t\|^2$. Define $\gamma_{d_t} := \frac{\langle -\nabla h(x^{(t)}), d_t \rangle}{L \|d_t\|^2}$ to be the step-size minimizing the RHS of the previous inequality. It is important to note that γ_{d_t} is not the step-size used in the algorithm obtained from line-search. It is used to only lower bound the progress obtained from the line-search step, since, plugging in γ_{d_t} in the smoothness inequality yields:

$$h(x^{(t)}) - h(x^{(t+1)}) = h(x^{(t)}) - h(x^{(t+1)}) \geq \frac{\langle -\nabla h(x^{(t)}), d_t \rangle^2}{2L \|d_t\|^2}. \quad (23)$$

We now split the proof depending on whether $\gamma_t < \gamma_t^{\max}$ or not:

(i) *First, suppose that $\gamma_t < \gamma_t^{\max}$.* We claim that we can use the step size from γ_{d_t} to lower

bound the progress even if γ_{d_t} is not a feasible step size (i.e. when $\gamma_{d_t} > 1$). To see this, note that the optimal solution of the line-search step is in the interior of the interval $[0, \gamma_t^{\max}]$. Define $x_\gamma := x^{(t)} + \gamma d_t$. Then, because $h(x_\gamma)$ is convex in γ , we know that $\min_{\gamma \in [0, \gamma_t^{\max}]} h(x_\gamma) = \min_{\gamma \geq 0} h(x_\gamma)$ and thus $\min_{\gamma \in [0, \gamma_t^{\max}]} h(x_\gamma) = h(x^{(t+1)}) \leq h(x_\gamma)$ for all $\gamma \geq 0$. In particular, $h(x^{(t+1)}) \leq h(x_{\gamma_{d_t}})$. Hence, we can use (23) to bound the progress per iteration as follows:

$$h(x^{(t)}) - h(x^{(t+1)}) \geq \frac{\langle -\nabla h(x^{(t)}), d_t^{\text{FW}} \rangle^2}{2L \|d_t^{\text{FW}}\|^2} \quad (\text{using smoothness}) \quad (24)$$

$$\geq \frac{\left\langle -\nabla h(x^{(t)}), \frac{d_{x^{(t)}}^\Pi}{\|d_{x^{(t)}}^\Pi\|} \right\rangle^2}{2LD^2} \quad (\text{choice of descent}) \quad (25)$$

$$\geq \frac{\mu}{LD^2} h(x^{(t)}), \quad (26)$$

where (26) follows Lemma 6.

(ii) We have a boundary case: $\gamma_t = \gamma_t^{\max}$. We further divide this case into two sub-cases:

- (a) First assume that $\gamma_{d_t} \leq \gamma_t^{\max}$ so that the step size from smoothness is feasible. Then, using the same argument as above we also have a $(1 - \frac{\mu}{LD^2})$ -geometric rate of decrease.
- (b) Finally assume that $\gamma_{d_t} > \gamma_t^{\max}$ and $d_t = d_t^{\text{FW}}$. Observe that $\gamma_{d_t} = \frac{\langle -\nabla h(x^{(t)}), d_t^{\text{FW}} \rangle}{L \|d_t^{\text{FW}}\|^2} > \gamma_t^{\max} = 1$ implies that $\langle -\nabla h(x^{(t)}), d_t^{\text{FW}} \rangle \geq L \|d_t^{\text{FW}}\|_2^2$. Hence, using the fact that $\gamma_t = \gamma_t^{\max} = 1$ in the smoothness inequality given previously, we have:

$$h(x^{(t)}) - h(x^{(t+1)}) \geq \left\langle -\nabla h(x^{(t)}), d_t^{\text{FW}} \right\rangle - \frac{L}{2} \|d_t^{\text{FW}}\|_2^2 \geq \frac{h(x^{(t)})}{2},$$

where the last inequality follows using the convexity of f as follows:

$$h(x^{(t)}) \leq \left\langle -\nabla h(x^{(t)}), x^* - x^{(t)} \right\rangle \leq \max_{v \in \mathcal{P}} \left\langle -\nabla h(x^{(t)}), v - x^{(t)} \right\rangle. \quad (27)$$

Hence, we get a geometric rate of decrease of $1/2$.

The iteration complexity stated in the theorem now follows using the above rate of decrease in the primal gap. \square

A Practical Variant of Shadow-CG. In the SHADOW-CG algorithm, we had to compute the shadow $d_{x^{(t)}}^\Pi$ every iteration to determine whether we take a FW step or enter TRACE-OPT. With the aim of improving the computational complexity of the the algorithm, we now propose a fast way to determine whether we can take a FW-step without computing the $d_{x^{(t)}}^\Pi$, while maintaining linear convergence. Recall from (15) that we have $\|\nabla h(x^{(t)})\| \geq \|d_{x^{(t)}}^\Pi\|$. Therefore, $\|d_{x^{(t)}}^\Pi\|$ can be approximated by $c\|\nabla h(x^{(t)})\|$, where $c \in (0, 1)$ is a scalar.

Algorithm 6 Shadow CG with Gradient test (SHADOW-CG²)

Input: Polytope $\mathcal{P} \subseteq \mathbb{R}^n$, function $f : P \rightarrow \mathbb{R}$, $x_0 \in P$, tuning parameter $c \in (0, 1)$, and accuracy parameter ε .

... same as Algorithm 5, except changing lines 4-7 as follows...

1: Initialize $\alpha = 1$

4: **if** $c\|\nabla h(x^{(t)})\| \leq \langle -\nabla h(x^{(t)}), d_t^{\text{FW}} \rangle$

5: $d_t := d_t^{\text{FW}}$ and $x^{(t+1)} := x^{(t)} + \gamma_t d_t$ ($\gamma_t \in [0, 1]$).

▷ use line-search

6: **else** $x^{(t+1)} := \text{TRACE-OPT}(x^{(t)}, \nabla h(x^{(t)}))$.

▷ trace projections curve

Return: $x^{(t+1)}$

We now propose our SHADOW-CG² algorithm, whose description is given in Algorithm 6. The algorithm is exactly the same as SHADOW-CG, but it now takes a FW step whenever $c\|\nabla h(x^{(t)})\| \leq \langle -\nabla h(x^{(t)}), d_t^{\text{FW}} \rangle$. Note that the smaller c is, the more the algorithm prioritizes FW steps. Thus, the scalar c serves as a tuning parameter for the algorithm that is used to trade off the computational complexity of the algorithm with the descent progress achieved per iteration. This is demonstrated by the following result:

Theorem 12. *Let $\mathcal{P} \subseteq \mathbb{R}^n$ be a polytope with diameter D and suppose that $f : P \rightarrow \mathbb{R}$ is L -smooth and μ -strongly convex over P . Then, the primal gap $h(x^{(t)}) := h(x^{(t)}) - h(x^*)$ of SHADOW-CG² decreases geometrically:*

$$h(x^{(t+1)}) \leq \left(1 - \min \left\{ \frac{1}{2}, \frac{c\mu}{LD^2}, \frac{\mu}{L} \right\}\right) h(x^{(t)}),$$

with each iteration of the SHADOW-CG² algorithm (assuming TRACE-OPT is a single step), where $c \in (0, 1)$ is the tuning parameter. Moreover, the running time to compute an ε -approximate solution is $O\left(\left(\frac{D^2}{c}L_O + \beta S\right)\frac{L}{\mu} \log\left(\frac{1}{\varepsilon}\right)\right)$, where β is the number of breakpoints of the parametric projections curve that the TRACE-OPT method visits, S is the number of calls to the shadow oracle (or in-face), and L_O is the time for linear optimization.

The same proof as that of Theorem 11 applies, after noting that $\|\nabla h(x)\| \geq \|d_{x^{(t)}}^\Pi\|$. We would remark that when the optimum x^* is constrained, $\|\nabla h(x^*)\|$ is lower bounded away from 0. Therefore, in the SHADOW-CG² algorithm it is preferable to choose the scalar c with small values to prioritize FW steps towards the end of the algorithm. In our computations, we did a grid-search over different values of c and found that $c = 0.1$ yielded an excellent performance as we discuss in Section 7.

Computational Complexity of AFW. Recall that the number of steps to get an ε -approximate solution for AFW is $O(\kappa(\frac{D}{\rho})^2 \log \frac{1}{\varepsilon})$, where κ , D , ρ are the condition number of the function, the diameter of the polytope, and the pyramidal-width, respectively. For the hypercube, $D^2 = n$ and $\rho^2 = 1/n$ [10]. Thus, the number of iterations to get an ε -approximate solution for AFW over the hypercube is $O(\kappa n^2 \log \frac{1}{\varepsilon})$. Each iteration takes $O(n^2)$ time, as it is $O(n)$ for linear optimization, $O(n^2)$ for maintaining a small active set using Caratheodory's Theorem, and therefore, the runtime complexity to get an ε -approximate solution using AFW for the hypercube is $O(\kappa n^4 \log \frac{1}{\varepsilon})$. For the

	AFW	Shadow-Walk	Shadow-CG
Iterations	$O(\kappa(D/\rho)^2 \log \frac{1}{\epsilon})$	$O(\kappa \log 1/\epsilon)$	$O(\kappa D^2 \log 1/\epsilon)$
Hypercube ($D^2 = n, \rho^2 = 1/n$)	$O(\kappa n^2 \log 1/\epsilon)$	$O(\kappa \log 1/\epsilon)$	$O(\kappa n \log 1/\epsilon)$
Simplex ($D^2 = 2, \rho^2 = 1/n$)	$O(\kappa n \log 1/\epsilon)$	$O(\kappa \log 1/\epsilon)$	$O(\kappa \log 1/\epsilon)$
Running Time			
Runtime complexity for Hypercube	$O(\kappa n^4 \log 1/\epsilon)$	$O(\kappa n^2 \log 1/\epsilon)$	$O(\kappa n^3 \log 1/\epsilon)$
Runtime complexity for Simplex	$O(\kappa n^3 \log 1/\epsilon)$	$O(\kappa n^3 \log 1/\epsilon)$	$O(\kappa n^3 \log 1/\epsilon)$

Table 1: Comparison between iteration complexity and runtime complexity for AFW (away-step Frank-Wolfe), SHADOW-WALK, and SHADOW-CG over the simplex and hypercube, where κ is the condition number of the function. We obtain a provable reduction of runtime complexity over the hypercube by using SHADOW-WALK, and reduction in the iteration complexity over the simplex, compared to AFW.

simplex, we have $D^2 = 2$ and $\rho^2 = 1/n$ [10]. Similar to the hypercube, the cost of each iteration of AFW over the simplex is $O(n^2)$, which implies that the runtime complexity to get an ϵ -approximate solution for the simplex using AFW is $O(\kappa n^3 \log \frac{1}{\epsilon})$.

On the other hand, the number of iterations to get an ϵ -approximate solution for SHADOW-WALK and SHADOW-CG is $O(\kappa \log \frac{1}{\epsilon})$ and $O(\kappa D^2 \log \frac{1}{\epsilon})$ respectively. Every iteration of both algorithms can in the worst case enter the TRACE-OPT procedure every iteration, which takes $O(n^2)$ and $O(n^3)$ time for the hypercube and simplex, respectively. Thus, for the hypercube, the running time complexity to get an ϵ -approximate solution for SHADOW-WALK and SHADOW-CG is $O(\kappa n^2 \log \frac{1}{\epsilon})$ and $O(\kappa n^3 \log \frac{1}{\epsilon})$ respectively. For the simplex, the running time complexity to get an ϵ -approximate solution for SHADOW-WALK and SHADOW-CG remains $O(\kappa n^3 \log \frac{1}{\epsilon})$, though the iteration complexity reduces. These comparisons become much starker when a scaled simplex is considered instead, as its pyramidal width can be reduced to be arbitrarily small. We summarize these complexity results in Table 1, and the runtime improvements will also be reflected in the computations in the next section.

7 Computations

We implemented all algorithms in Python 3.5. We used Gurobi 9 [42] as a black box solver for some of the oracles assumed in the paper. All experiments were performed on a 16-core machine with Intel Core i7-6600U 2.6-GHz CPUs and 256GB of main memory^{¶¶}. We are required to solve the following subproblems:

- (i) **Linear optimization:** Compute $v = \arg \min_{x \in \mathcal{P}} \langle c, x \rangle$ for any $c \in \mathbb{R}^n$. We elaborate on the implementation of the LO subproblems later on as it is dependent on the application.
- (ii) **Shadow computation:** Given any point $x \in \mathcal{P}$ and direction $w \in \mathbb{R}^n$, compute $d_x^{\text{II}}(w)$. For the shadow oracle, we solve the problem $d_x^{\text{II}}(w) = \arg \min_d \{ \| -\nabla h(x) - d \|^2 : A_{I(x)} d \leq 0 \}$ using

^{¶¶}This code and datasets used for our computations are available at <https://github.com/hassanmortagy/Walking-in-the-Shadow>.

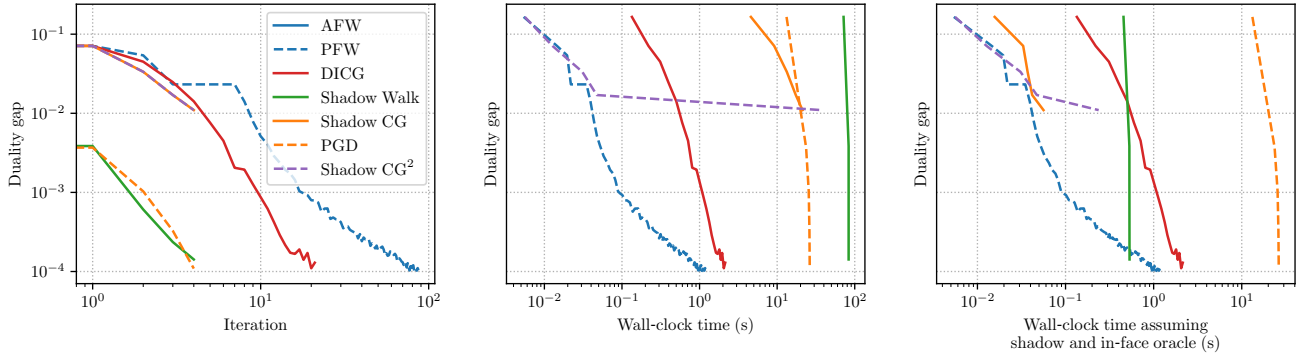


Figure 4: Duality gap for the video co-localization problem. Left plot compares iteration count, middle and right plots compare wall-clock time with and without access to shadow oracle. We removed PGD from the rightmost plot for a better comparison as it takes significantly more time due to the projection step and skews the plot.

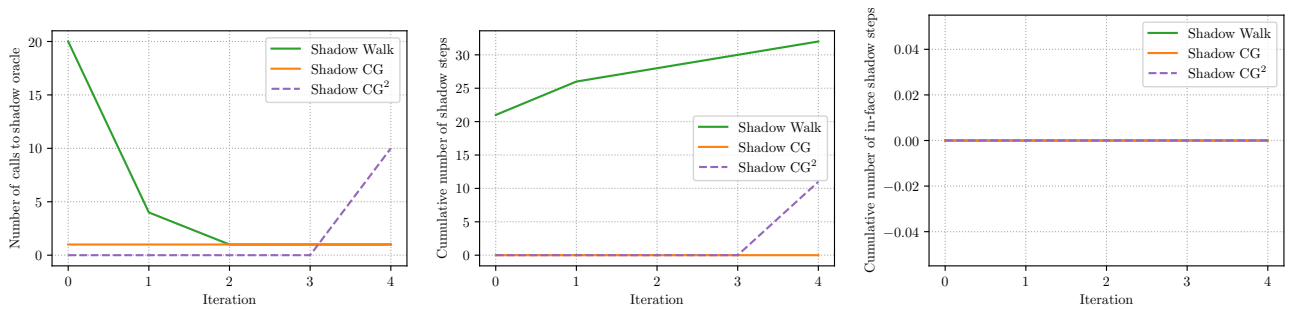


Figure 5: Oracle calls for the video Co-localization problem. Left plot shows the number of shadow oracles calls made per iteration by SHADOW-WALK, SHADOW-CG, and SHADOW-CG². Note that in the plot we see that SHADOW-CG makes one shadow oracle call every iteration, whereas SHADOW-CG² does not. The middle plot compares the cumulative number of shadow steps taken. Right plot compares the cumulative number of in-face shadow steps taken.

Gurobi^{***} in Section 7.1. However, in Section 7.2, we use the SHADOW-SIMPLEX algorithm (Algorithm 3) to compute the shadow and trace the projections curve.

(iii) **Feasibility:** For any $x \in \mathcal{P}$ and direction $d \in \mathbb{R}^n$, evaluate $\gamma^{\max} = \max\{\delta : x + \delta d \in \mathcal{P}\} = \min_{j \in J(x): \langle a_j, d \rangle > 0} \frac{b_j - \langle a_j, x \rangle}{\langle a_j, d \rangle}$. This problem could be efficiently solved as we consider polytopes with a polynomial number of constraints.

(iv) **Line-search:** Given any point $x \in \mathcal{P}$ and direction $d \in \mathbb{R}^n$, solve the one-dimensional problem $\min_{\gamma \in [0, \gamma^{\max}]} h(x + \gamma d)$. To solve that problem, we utilize a bracketing method^{†††} for line search.

Finally, to compute $\hat{\lambda}$ in step 5 of the TRACE-OPT algorithm, we utilize the procedure of solving a

^{***}This could also be computed approximately using the *matching pursuit* approach with FW of Locatello et. al [43], which extends FW to optimize convex function over cones (and not just polytopes). However, for our preliminary computations we chose Gurobi due its robustness and exact solutions.

^{†††}We specifically use golden-section search that iteratively reduces the interval locating the minimum (see e.g. [27]).

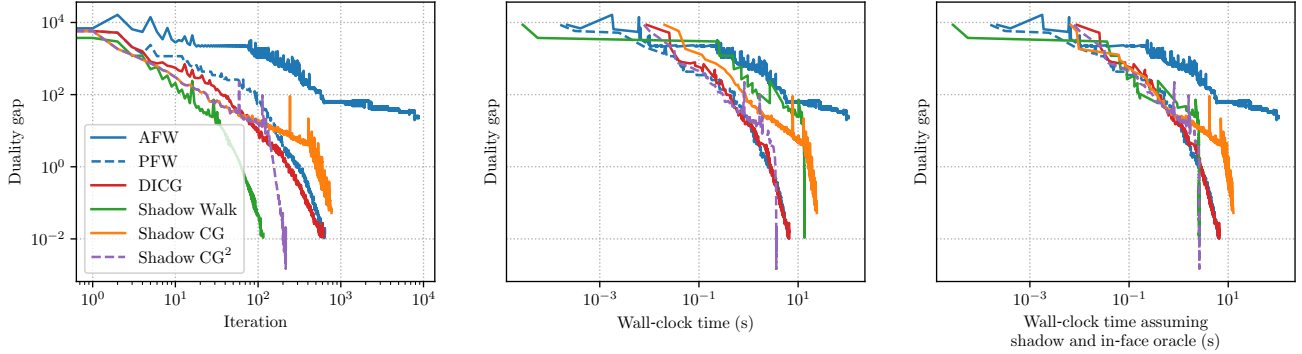


Figure 6: Duality gaps for the Lasso regression problem: Left plot compares iteration count, middle and right plots compare wall-clock time with and without access to shadow oracle.

linear program outlined in Remark 2.

7.1 Video Co-localization

The first application we consider is the video co-localization problem from computer vision, where the goal is to track an object across different video frames. We used the YouTube-Objects dataset^{†††} and the problem formulation of Joulin et. al [5]. This consists of minimizing a quadratic function $h(x) = \frac{1}{2}x^\top Ax + b^\top x$, where $x \in \mathbb{R}^{660}$, $A \in \mathbb{R}^{660 \times 660}$ and $b \in \mathbb{R}^{660}$, over a flow polytope, the convex hull of paths in a network. Our linear minimization oracle over the flow polytope amounts to computing a shortest path in the corresponding directed acyclic graph. We now present the computational results.

We find that SHADOW-CG and SHADOW-CG² have a lower iteration count than other CG variants DICG, AFW and PFW (slightly higher than PGD) for this experiment. In particular, SHADOW-CG² takes slightly more iterations than SHADOW-CG, but takes significantly less wall-clock time (i.e., close to CG) without assuming oracle access to shadow, i.e., when we include the time needed to compute the shadow in our running times, thus obtaining the best of both worlds. Moreover, without assuming oracle access to the shadow computation, SHADOW-CG improves on the wall-clock time compared to PGD and SHADOW-WALK (close to CG). We also find that assuming access to shadow oracle, the SHADOW-CG algorithm outperforms the CG variants both in iteration count and wall-clock time. As is common in analyzing FW variants, we compare these different algorithms with respect to the duality gap $\langle -\nabla h(x^{(t)}), v^{(t)} - x^{(t)} \rangle$ (27) in Figure 4.

7.2 Lasso Regression

The second application we consider is the Lasso regression problem, i.e., ℓ_1 -regularized least squares regression. This consists of minimizing a quadratic function $h(x) = \|Ax - b\|^2$ over a scaled ℓ_1 -

^{†††}We obtained the data from <https://github.com/Simon-Lacoste-Julien/linearFW>.

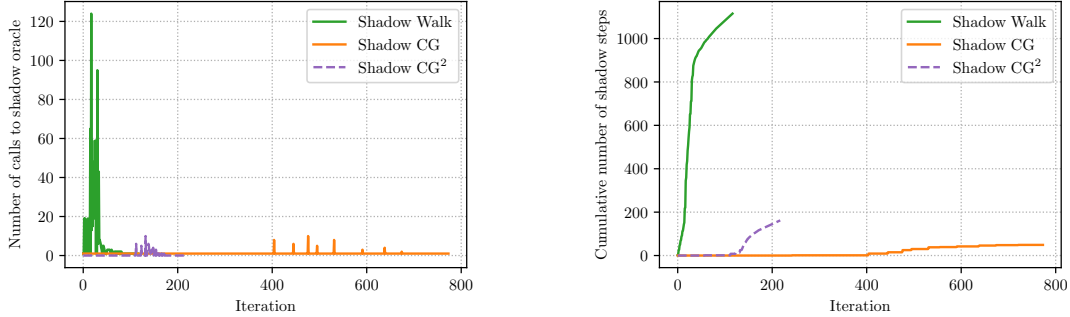


Figure 7: Left: Comparing the number of shadow oracles calls made per iteration by SHADOW-WALK, SHADOW-CG, and SHADOW-CG² in the Lasso regression instance. Right: Comparing the cumulative number of shadow steps taken. Here, we find that SHADOW-WALK, SHADOW CG and SHADOW-CG² algorithms do not take any in-face steps and the number of iterations spent in the TRACE-OPT procedure matches the $O(n)$ bound we prove in Theorem 6.

ball. The ℓ_1 ball could be formulated as a scaled probability simplex using an extended formulation (see for example [37]). We use this formulation that we can invoke the SHADOW-SIMPLEX algorithm (Algorithm 3) to compute the shadow and trace the projections curve.

We considered a random Gaussian matrix $A \in \mathbb{R}^{50 \times 100}$ and a noisy measurement $b = Ax^*$ with x^* being a sparse vector with 25 entries ± 1 , and some additive noise. Linear minimization over the ℓ_1 -ball, simply amounts to selecting the column of A with best inner product with the residual vector $Ax - b$. In these experiments, we observe that our algorithms SHADOW-WALK and SHADOW-CG algorithms are superior both in an iteration count and wall-clock time, and outperform all other CG variants; this is without assuming access to shadow. Moreover, assuming access to a shadow oracle, those improvements are even more pronounced. We demonstrate computationally that the number of iterations spent in the TRACE-OPT procedure matches the $O(n)$ bound we prove in Theorem 6 and that we do not have in-face steps. Moreover, we also find that the addition of FW steps causes the SHADOW CG and SHADOW-CG² algorithms to take a significantly smaller number of shadow steps than SHADOW-WALK does.

8 Conclusion

In this work, we showed connections between various descent directions for constrained minimization, such as for Frank-Wolfe direction, away-steps, pairwise steps. Further, we characterized the structure of the projections curve, and showed that it consists of two directions: the shadow, and the in-face shadow. Using this structure, we showed that the simplex and hypercube enjoy a linear number of breakpoints in the projections curve. We analyzed the continuous-time dynamics of moving along the shadow, and showed a possible discretion using SHADOW-WALK. Using the insight that Frank-Wolfe vertices are simply greedy projections, we proposed SHADOW-CG (and its practical variant SHADOW-CG²) which can switch between taking the Frank-Wolfe direction and shadow-

steps as needed, to obtain linear convergence. SHADOW-CG enjoys a linear rate of convergence, which depends on affine-invariant geometric constants only. These results answer the key question considered in this work about optimal descent directions for constrained minimization.

We hope that this analysis helps inform future studies, especially those that improve oracle running times for computing the shadow, as well as machine learning to find good descent directions. Although we focused on analyzing descent directions, these ideas can be applied to accelerated proximal methods [19, 44] as well, simply due to our ability to unpack the projections curve through TRACE-OPT. We leave exploring such extensions to future work. Further, we showed linear bounds on the number of breakpoints for two simple polytopes, by analyzing the KKT conditions for the breakpoints. Though we can only show an $O(2^m)$ bound for the number of breakpoints in general, we conjecture that it should be $O(m)$, where m is the number of facet-defining inequalities.

A The TRACE-OPT Algorithm

We now present our TRACE-OPT Algorithm, which chains together consecutive short descent steps and uses line-search until it minimizes the function h over the linear segments of projections curve (until we hit the step-size $1/L$, where L is the smoothness constant). That way we are guaranteed progress that is at least as that of a single PGD step with fixed $1/L$ step size. One important property of TRACE-OPT is that it only requires one gradient oracle call. The complete description of the algorithm is give below in Algorithm 7.

B Deriving the Structure of the Projections Curve using Complementary Pivot Theory

The structure of parametric quadratic programs has been well-studied. In this section, we show how one can reduce the problem of computing the projections curve $g(\lambda)$ using complementary pivot theory. The exposition of this section is inspired from [25, 24]. Consider the following fundamental problem: Given real vectors $q, z \in \mathbb{R}^n$ and matrix $M \in \mathbb{R}^{n \times n}$ find vectors w and z that satisfy the conditions:

$$\begin{aligned} w &= q + MZ, \\ z^\top w &= 0, \\ w, z &\geq 0. \end{aligned} \tag{LC}$$

The *quadratic programming problem* is typically stated as

$$\begin{aligned} \min \quad & \frac{1}{2}x^\top Dx + c^\top x \\ \text{s.t.} \quad & Ax \leq b, \\ & x \geq 0, \end{aligned} \tag{QP}$$

where $D \in \mathbb{R}^{n \times n}$ is symmetric and positive semi-definite. Notice that the problem of evaluating $g(\lambda)$

Algorithm 7 Tracing Projections Curve Optimally: TRACE-OPT(x, w)

Input: Polytope $\mathcal{P} \subseteq \mathbb{R}^n$, L -smooth function $h : \mathcal{P} \rightarrow \mathbb{R}$ and initialization $x \in \mathcal{P}$

```

1: Let  $x^{(0)} = x$  and  $\gamma^{\text{total}} = 0$ . ▷ fix starting point and initialize total step size
2: Compute  $d_x^\Pi := \lim_{\epsilon \downarrow 0} \frac{\Pi_{\mathcal{P}}(x - \epsilon \nabla h(x^{(0)})) - x}{\epsilon}$ .
3: while  $d_x^\Pi \neq 0$  do ▷ check if we are at endpoint
4:   if  $\langle x^{(0)} - \gamma^{\text{total}} \nabla h(x^{(0)}) - x, d_x^\Pi \rangle = 0$  then ▷ determine if we take shadow step
5:     Compute  $\gamma^{\text{max}} = \max\{\delta \mid x + \delta d_x^\Pi \in \mathcal{P}\}$  ▷ feasibility line-search in shadow direction
6:     Set  $d = d_x^\Pi$ . ▷ take shadow step
7:   else
8:      $\hat{d}_x^\Pi, \gamma^{\text{max}} = \text{TRACE-IN-FACE}(x^{(0)}, x, \nabla h(x^{(0)}), \gamma^{\text{total}})$ . ▷ in-face step
9:     set  $d = \hat{d}_x^\Pi$ .
10:  end if
11:  if  $\gamma^{\text{total}} + \gamma^{\text{max}} \geq 1/L$  and  $d \neq 0$  then
12:    Compute  $\gamma^* \in \arg \min_{\gamma \in [0, \gamma^{\text{max}}]} h(x + \gamma d)$ . ▷ optimality line-search
13:    Update  $x = x + \gamma^* d$ 
14:    break ▷ we made sufficient descent progress
15:  else
16:    Update  $x = x + \gamma^{\text{max}} d$  and  $\gamma^{\text{total}} = \gamma^{\text{total}} + \gamma^{\text{max}}$ . ▷ keep track of total step-size accrued
17:    Recompute  $d_x^\Pi := \lim_{\epsilon \downarrow 0} \frac{\Pi_{\mathcal{P}}(x - \epsilon \nabla h(x^{(0)})) - x}{\epsilon}$ 
18:  end if
19: end while

```

Return: x

for any $\lambda \in \mathbb{R}_+$ is a special case of (QP). Indeed,

$$\begin{aligned}
 g(\lambda) = \arg \min \quad & \frac{1}{2} \|x_0 - \lambda \nabla h(x_0) - x\|_2^2 & \arg \min \quad & \frac{1}{2} \|x\|_2^2 + \langle x_0 - \lambda \nabla h(x_0), x \rangle \\
 \text{s.t. } & Ax \leq b, & \text{s.t. } & Ax \leq b, \\
 & x \geq 0, & & x \geq 0.
 \end{aligned} \tag{28}$$

Therefore, by setting $D = I$ and $c = x_0 - \lambda \nabla h(x_0)$ in (QP), we recover the problem of computing $g(\lambda)$. We next show how can reduce (QP) to (LC).

For any quadratic programming problem (QP), define u and v by

$$u = Dx + c + A^\top y, \quad v = b - Ax. \tag{29}$$

Using the KKT conditions, we know that a vector \tilde{x} yields a minimum of (QP) if only if there exists a vector \tilde{y} and vectors \tilde{u}, \tilde{v} given by (11) for $x = \tilde{x}$ in (29) satisfying:

$$\begin{aligned}
 \tilde{x} \geq 0, \quad \tilde{u} \geq 0, \quad \tilde{v} \geq 0, \quad \tilde{y} \geq 0, \\
 \tilde{x}^\top \tilde{u} = 0, \quad \tilde{y}^\top \tilde{v} = 0.
 \end{aligned} \tag{30}$$

Therefore, the problem of solving a quadratic program leads to a search for solution of the

system:

$$\begin{aligned} u &= Dx + c + A^\top y, & v &= b - Ax, & x^\top u + y^\top v &= 0 \\ x, y &\geq 0, & u, v &\geq 0 \end{aligned}$$

In particular, by setting

$$w = \begin{pmatrix} u \\ v \end{pmatrix}, \quad q = \begin{pmatrix} c \\ -b \end{pmatrix}, \quad M = \begin{pmatrix} D & -A^\top \\ A & 0 \end{pmatrix},$$

one can reduce the quadratic programming problem to the linear complementarity problem (LC).

There exists an iterative algorithm called the *complementary pivot algorithm* and is very similar to the Simplex method, which can solve (LC) under some conditions on the matrix M . If M is positive-semi definite for instance then the *complementary pivot algorithm* can solve (LC) [24]. In our case,

$$M = \begin{pmatrix} D & -A^\top \\ A & 0 \end{pmatrix},$$

which can easily be verified to be positive semi-definite. Indeed, for any $x \in \mathbb{R}^n$

$$\begin{aligned} x^\top Mx &= \begin{pmatrix} x_1 \\ x_2 \end{pmatrix} M = \begin{pmatrix} D & -A^\top \\ A & 0 \end{pmatrix} \begin{pmatrix} x_1 \\ x_2 \end{pmatrix} = x_1^\top Dx_1 + x_2^\top Ax_1 - x_1^\top Ax_2 \\ &= x_1^\top Dx_1 \geq 0, \end{aligned}$$

since D is assumed to be positive semi-definite. Therefore, the key takeaway is that we can solve any quadratic problem using the complementary pivot algorithm.

Finally, there is a parametric version of (LC) defined as follows:

$$\begin{aligned} w - Mz &= q(\lambda) := s + \lambda \bar{s} \\ z^\top w &= 0 \\ w, z &\geq 0 \end{aligned} \tag{PLC}$$

Moreover, there exists an algorithm, the *parametric complementary pivot algorithm* that can solve (PLC) for all values of λ [24], i.e. it traces the piecewise linear solution path generated by considering all values of λ . So, by setting

$$w = \begin{pmatrix} u \\ v \end{pmatrix}, \quad M = \begin{pmatrix} D & -A^\top \\ A & 0 \end{pmatrix} s = \begin{pmatrix} x_0 \\ -b \end{pmatrix}, \quad \bar{s} = \begin{pmatrix} -\nabla h(x_0) \\ -0 \end{pmatrix},$$

in (PLC) we can solve (B) for any λ . Therefore, one can also trace the projections curve using the parametric complementary pivot algorithm.

C Missing proofs for Section 3

C.1 Proof of Theorem 5

Theorem 5 (Breakpoints for the Hypercube). *Consider the n -dimensional hypercube $\mathcal{H}_n := \{x \in \mathbb{R}^n \mid 0 \leq x_i \leq 1 \forall i \in [n]\}$ and fix $x_0 \in \mathcal{H}_n$. Then, the projections curve $g(\lambda) = \Pi_P(x_0 - \lambda w)$ has only $O(n)$ breakpoints (for $\lambda \geq 0$).*

Proof. For notational brevity, we let $d_{x_{i-1}}^{\Pi} := d_{x_{i-1}}^{\Pi}(w)$ for all $i \geq 1$. First, note that for the hypercube, the shadow could be computed in closed form in $O(n)$ time, using

$$[d_x^{\Pi}(w)]_i = \begin{cases} 0 & \text{if } i \in I_1 \text{ and } [-w]_i \leq 0; \\ 0 & \text{if } i \in I_2 \text{ and } [-w]_i \geq 0; \\ [-w]_i & \text{otherwise.} \end{cases} \quad (31)$$

This is because, $d_{x_{i-1}}^{\Pi}$ is given by a projection onto the tangent cone at x given by $T_{\mathcal{H}_n}(x) = \{d \in \mathbb{R}^n \mid d_i \geq 0 \text{ if } x_i = 0, d_i \leq 0 \text{ if } x_i = 1\}$: $d_x^{\Pi}(w) = \arg \min_{d \in T_{\mathcal{H}_n}(x)} \|-w - d\|^2$, and therefore,

$$d_x^{\Pi}(w) = \left\{ \begin{array}{l} \arg \min_{d \in \mathbb{R}^n} \|-w - d\|^2 \\ \text{subject to} \quad \begin{array}{ll} d_i \geq 0 & \text{if } i \in I_1 \\ -d_i \geq 0 & \text{if } i \in I_2 \end{array} \end{array} \right\};$$

We next show that $\langle x_0 - \lambda_{i-1}^- w - x_{i-1}, d_{x_{i-1}}^{\Pi} \rangle = 0$ for all $i \geq 1$ by (strong) induction on i , which using Theorem 3 implies that we only take shadow steps in $\text{TRACE}(x_0, x_{i-1}, w, \lambda_{i-1}^-)$. For the base case when $i = 1$, we know using Remark 1 (a) that $\langle x_0 - \lambda_0^- w - x_0, d_{x_0}^{\Pi} \rangle = 0$ and the first segment of the projections curve could be obtained using a maximal shadow-step. This establishes the base case. For the inductive step, assume that $\langle x_0 - \lambda_j^- w - x_j, d_{x_j}^{\Pi} \rangle = 0$ for all $j \leq i - 1$ and we show that

$$\langle x_0 - \lambda_i^- w - x_i, d_{x_i}^{\Pi} \rangle = \sum_{k=1}^n [x_0 - \lambda_i^- w - x_i]_k \times [d_{x_i}^{\Pi}]_k = 0. \quad (32)$$

In particular, we will show that for any $k \in [n]$ where $[d_{x_i}^{\Pi}]_k = [-w]_k \neq 0$, then $[x_0 - \lambda_i^- w - x_i]_k = 0$, which proves (32).

By the induction hypothesis and Theorem 3, we know that have only taken shadow steps until the breakpoint x_i , and thus

$$x_i = x_0 + \sum_{j=0}^{i-1} x_0 + (\lambda_{j+1}^- - \lambda_j^+) d_{x_j}^{\Pi} = x_0 + \sum_{j=0}^{i-1} (\lambda_{j+1}^- - \lambda_j^-) d_{x_j}^{\Pi}, \quad (33)$$

where the second equality uses the fact that $\lambda_j^- = \lambda_j^+$ for all $j \leq i - 1$ using Remark 2 since we did not take any in-face steps by induction. Furthermore, we claim that $[d_{x_j}^{\Pi}]_k = [-w]_k$ for all $j \leq i - 1$.

Suppose for a contradiction, that our claim is false, i.e. $[d_{x_j}^{\Pi}]_k = 0$ for some $j \leq i - 1$. Then by the fact that we have only take shadow steps by induction and (31), it follows that $[d_{x_l}^{\Pi}]_k = 0$ for all l satisfying $j \leq l \leq i - 1$. Therefore,

$$[x_i]_k = [x_0]_k + \sum_{j=0}^{i-1} (\lambda_{j+1}^- - \lambda_j^-) [d_{x_j}^{\Pi}]_k = [x_j]_k + \sum_{l=j}^{i-1} (\lambda_{l+1}^- - \lambda_l^-) [d_{x_l}^{\Pi}]_k = [x_j]_k,$$

where we used the fact that $[x_j]_k = x_0 + \sum_{l=0}^{j-1} (\lambda_{l+1}^- - \lambda_l^-) [d_{x_l}^{\Pi}]_k$ by induction. Since, $[x_i]_k = [x_j]_k$, this implies that $[x_i]_k$ and thus $[d_{x_i}^{\Pi}]_k = 0$, which is a contradiction to our assumption that $[d_{x_i}^{\Pi}]_k = [-w]_k \neq 0$.

Thus using the previous claim and (33) we have

$$\begin{aligned} [x_0 - \lambda_i^- w - x_i]_k &= [x_0]_k - \lambda_i^- [w]_k - [x_0]_k - \sum_{j=0}^{i-1} (\lambda_{j+1}^- - \lambda_j^-) [d_{x_j}^{\Pi}]_k \\ &= [x_0]_k - \lambda_i^- [w]_k - [x_0]_k - \sum_{j=0}^{i-1} (\lambda_{j+1}^- - \lambda_j^-) [-w]_k \\ &= \lambda_i^- [-w]_k - (\lambda_i^- - \lambda_0^-) [-w]_k \\ &= \lambda_i^- [-w]_k - \lambda_i^- [-w]_k \quad (\lambda_0^- = 0) \\ &= 0, \end{aligned}$$

which proves (32) and completes the induction. We have proven that in TRACE, we only take shadow steps. In such steps, we move maximally along the shadow, and so in every iteration a coordinate of x_i becomes tight (i.e. $[x_j]_k = 0$ or $[x_j]_k = 1$). Since, once coordinate is tight, it remains tight as proven earlier, and we are only taking maximal shadow steps, it will take $O(n)$ iterations until $d_{x_j}^{\Pi} = 0$, which implies that we reached the endpoint of the projections curve using Theorem 3. \square

C.2 Proof of Lemma 4

Lemma 4. *Consider any $x \in \Delta_n$ and any direction $w \in \mathbb{R}^n$, Then, the output of SHADOW-SIMPLEX(x, w) (Algorithm 3) is $d_x^{\Pi}(w)$. Moreover, the running time of the algorithm is $O(n \log n + n^2)$ time.*

Proof. Recall that

$$d_x^{\Pi}(w) = \arg \min_{d \in T_{\Delta_n}(x)} \| -w - d \|^2,$$

where $T_{\Delta_n}(x)$ is the tangent cone at x given by $\{d \in \mathbb{R}^n \mid d_i \geq 0 \text{ if } x_i = 0, \sum_{i=1}^n d_i = 0\}$. Let $I := \{i \in [n] \mid x_i = 0\}$ and $J := \{i \in [n] \mid x_i > 0\}$. Therefore,

$$d_x^{\Pi}(w) = \left\{ \arg \min_{d \in \mathbb{R}^n} \| -w - d \| \mid \sum_{i=1}^n d_i = 0, d_i \geq 0 \forall i \in I \right\}. \quad (34)$$

Let $I^* = \{i \in I \mid d_x^{\Pi}(w)_i = 0\}$ be the index-set of coordinates where the shadow $d_x^{\Pi}(w)_i = 0$. As in

Algorithm 3, for simplicity of notation, we let $g := -w$. Then, (34) is equivalent to*

$$d_x^\Pi(w) = \left\{ \arg \min_{d \in \mathbb{R}^n} \|g - d\|^2 \mid \sum_{i=1}^n d_i = 0, d_i = 0 \text{ for all } i \in I^* \right\}. \quad (35)$$

Let C denote the feasible region of (35). Furthermore, let r be a vector defined as follows:

$$r_i = \begin{cases} 0 & \text{if } i \in I^*; \\ 1 & \text{otherwise.} \end{cases}$$

Assuming we know I^* , we can solve (35) in closed form as follows since it is just a Euclidean projection onto $\mathbb{1}^\top d = 0$ with the restriction that $d_i = 0$ for all $i \in I^*$.

$$d := g \odot r - \frac{\langle g, r \rangle}{\|r\|^2} r = d_x^\Pi(w). \quad (36)$$

We finally claim that the u_x computed by Algorithm 3 satisfies

$$u_x = r. \quad (37)$$

which complete the proof. We prove (37) by showing that $I' := \{i \in I \mid [u_x]_i = 0\} = I^*$. By the initialization of u in line 2 of the Algorithm, we have that $[u_x]_i = 1$ for all $i \in J$. It remains to show that $[u_x]_i = 1$ for all $I \setminus I^*$. To do that, it suffices to prove that for any $i, j \in I$, if $g_i \geq g_j$, then $[d_x^\Pi(w)]_i \geq [d_x^\Pi(w)]_j$, since in Algorithm 3 we sort I to be consistent with ordering g in decreasing order, and then searching for I^* greedily based on that order. Suppose on the contrary that $g_i \geq g_j$ for some $i, j \in I$ but $[d_x^\Pi(w)]_i < [d_x^\Pi(w)]_j$ for $i < j$. Let $\tilde{d}_x^\Pi(w)$ be the direction obtained by exchanging $[d_x^\Pi(w)]_i$ and $[d_x^\Pi(w)]_j$. Then, by construction, we have that $\tilde{d}_x^\Pi(w)$ is feasible (34). Moreover,

$$\begin{aligned} \|g - d_x^\Pi(w)\|^2 - \|g - \tilde{d}_x^\Pi(w)\|^2 &= (g_i - [d_x^\Pi(w)]_i)^2 + (g_j - [d_x^\Pi(w)]_j)^2 - (g_i - [\tilde{d}_x^\Pi(w)]_i)^2 - (g_j - [\tilde{d}_x^\Pi(w)]_j)^2 \\ &= -2(g_i)([d_x^\Pi(w)]_i) - 2(g_j)([d_x^\Pi(w)]_j) + 2(g_i)([\tilde{d}_x^\Pi(w)]_i) + 2(g_j)([\tilde{d}_x^\Pi(w)]_j) \\ &= 2([d_x^\Pi(w)]_j - [d_x^\Pi(w)]_i)(g_i - g_j) \\ &\geq 0, \end{aligned}$$

which contradicts the optimality of $d_x^\Pi(w)$.

Finally, regarding the running times, Algorithm 3 requires an initial sort of g , which requires $O(n \log n)$ time, and then running the for-loop in line 5 which has at most n iterations, where in every iteration we do the computation in (36), which takes $O(n)$ time. This gives a total running time of $O(n \log n + n^2)$ as claimed. \square

*See Lemma 2 in [32] about reducing the optimization problem to the optimal face if this is not clear.

C.3 Proof of Theorem 6

Theorem 6 (Breakpoints for the Simplex). *Let $\Delta_n := \{x \in \mathbb{R}^n \mid \sum_{i=1}^n x_i = 1, x_i \geq 0 \forall i \in [n]\}$ denote the $(n-1)$ -dimensional simplex and fix $x_0 \in \Delta_n$. Then, the projections curve $g(\lambda) = \Pi_P(x_0 - \lambda w)$ has only $O(n)$ breakpoints (for $\lambda \geq 0$).*

Proof. For notational brevity, we let $d_{x_{i-1}}^\Pi := d_{x_{i-1}}^\Pi(w)$ for all $i \geq 1$ and let $g := -w$ (similar to Algorithm 3). We will prove this lemma by first showing that $\langle x_0 + \lambda_{i-1}^- g - x_{i-1}, d_{x_{i-1}}^\Pi \rangle = 0$ for all $i \geq 1$. At the start point of the curve when $i = 1$, we know using Remark 1 (a) that $\langle x_0 + \lambda_0^- g - x_0, d_{x_0}^\Pi \rangle = 0$ and the first segment of the projections curve could be obtained using a maximal shadow-step. Therefore, using Theorem 3, we have that $x_1 = x_0 + \lambda_1^- d_{x_0}^\Pi = x_0 + (\lambda_1^- - \lambda_0^-) d_{x_0}^\Pi$. Now, consider the next segment of the projections curve starting at x_1 . We will now prove that we again take a maximal shadow step to obtain the next segment of the curve, by showing that

$$\langle x_0 + \lambda_1^- g - x_1, d_{x_1}^\Pi \rangle = \langle x_0 + (\lambda_1^- - \lambda_0^-)g - x_0 - (\lambda_1^- - \lambda_0^-)d_{x_0}^\Pi, d_{x_1}^\Pi \rangle = (\lambda_1^- - \lambda_0^-) \langle g - d_{x_0}^\Pi, d_{x_1}^\Pi \rangle = 0,$$

i.e., by proving that $\langle g - d_{x_0}^\Pi, d_{x_1}^\Pi \rangle = 0$. To that end, using Algorithm 3, we know that

$$d_{x_0}^\Pi = g \odot u_{x_0} - \frac{\langle g, u_{x_0} \rangle}{\|u_{x_0}\|^2} u_{x_0} \quad \text{and} \quad d_{x_1}^\Pi = g \odot u_{x_1} - \frac{\langle g, u_{x_1} \rangle}{\|u_{x_1}\|^2} u_{x_1}. \quad (38)$$

Let $\text{supp}(u_{x_1}) := \{i \in [n] \mid [u_{x_1}]_i = 1\}$. Then, since x_1 is obtained by moving maximally along $d_{x_0}^\Pi$ from x_0 , we also know that[†]

$$\text{supp}(u_{x_1}) \subset \text{supp}(u_{x_0}) \implies u_{x_1} \odot u_{x_0} = u_{x_1}, \langle u_{x_1}, u_{x_0} \rangle = \|u_{x_1}\|^2, \quad (39)$$

which further implies that $\langle u_{x_0}, g \odot u_{x_1} \rangle = \langle u_{x_1}, g \odot u_{x_0} \rangle = \langle u_{x_1}, g \rangle$. Putting everything together:

$$\begin{aligned} \langle g - d_{x_0}^\Pi, d_{x_1}^\Pi \rangle &= \left\langle g - g \odot u_{x_0} + \frac{\langle g, u_{x_0} \rangle}{\|u_{x_0}\|^2} u_{x_0}, g \odot u_{x_1} - \frac{\langle g, u_{x_1} \rangle}{\|u_{x_1}\|^2} u_{x_1} \right\rangle \\ &= \left\langle g - g \odot u_{x_0}, g \odot u_{x_1} - \frac{\langle g, u_{x_1} \rangle}{\|u_{x_1}\|^2} u_{x_1} \right\rangle + \frac{\langle g, u_{x_0} \rangle}{\|u_{x_0}\|^2} \left\langle u_{x_0}, g \odot u_{x_1} - \frac{\langle g, u_{x_1} \rangle}{\|u_{x_1}\|^2} u_{x_1} \right\rangle \end{aligned} \quad (40)$$

$$= \|g \odot u_{x_1}\|^2 - \frac{\langle g, u_{x_1} \rangle^2}{\|u_{x_1}\|^2} - \|g \odot u_{x_1}\|^2 + \frac{\langle g, u_{x_1} \rangle^2}{\|u_{x_1}\|^2} = 0 \quad (41)$$

where we used (39) in (40) and (41). Note that the only property we used to prove that $\langle g - d_{x_0}^\Pi, d_{x_1}^\Pi \rangle = 0$ is that $\text{supp}(u_{x_1}) \subset \text{supp}(u_{x_0})$; this will be important for the remainder of the proof.

[†]It is clear that $\text{supp}(u_{x_1}) \subseteq \text{supp}(u_{x_0})$ since x_0 lies in a higher dimensional face of the simplex containing x_0 (x_1 has more zero coordinates than x_0), and so computing the shadow at x_1 is a more constrained optimization problem than computing it at x_0 . However, equality cannot hold since x_1 is obtained by moving maximally along the shadow. In other words, if $\text{supp}(u_{x_1}) = \text{supp}(u_{x_0})$, then $d_{x_0}^\Pi = d_{x_1}^\Pi$, and since $d_{x_1}^\Pi$ is a feasible direction at x_1 by definition, we contradicts that x_1 is obtained by moving maximally along $d_{x_0}^\Pi$ from x_0 .

Therefore, using Theorem 3, we know that the next breakpoint:

$$x_2 = x_1 + (\lambda_2^- - \lambda_1^-)d_{x_1}^\Pi = x_0 + (\lambda_2^- - \lambda_1^-)d_{x_1}^\Pi + (\lambda_1^- - \lambda_0^-)d_{x_0}^\Pi, \quad (42)$$

and thus $\text{supp}(u_{x_2}) \subset \text{supp}(u_{x_1}) \subset \text{supp}(u_{x_0})$. Then, using (42) and the exact same calculation as above, we obtain

$$\begin{aligned} \langle x_0 + \lambda_2^- g - x_2, d_{x_2}^\Pi \rangle &= \langle x_0 + \lambda_2^- g - x_0 - (\lambda_2^- - \lambda_1^-)d_{x_1}^\Pi - (\lambda_1^- - \lambda_0^-)d_{x_0}^\Pi, d_{x_2}^\Pi \rangle \\ &= (\lambda_1^- - \lambda_0^-) \underbrace{\langle g - d_{x_0}^\Pi, d_{x_2}^\Pi \rangle}_{=0 \text{ since } \text{supp}(u_{x_2}) \subset \text{supp}(u_{x_0})} + (\lambda_2^- - \lambda_1^-) \underbrace{\langle g - d_{x_1}^\Pi, d_{x_2}^\Pi \rangle}_{=0 \text{ since } \text{supp}(u_{x_1}) \subset \text{supp}(u_{x_0})} = 0. \end{aligned}$$

Continuing inductively in this fashion, we have $\text{supp}(u_{x_i}) \subset \text{supp}(u_{x_{i-1}}) \subset \dots \subset \text{supp}(u_{x_0})$ for any breakpoint $i > 2$, and thus

$$\langle x_0 + \lambda_i^- g - x_i, d_{x_i}^\Pi \rangle = \left\langle x_0 + \lambda_i^- g - x_0 - \sum_{j=0}^{i-1} (\lambda_{j+1}^- - \lambda_j^-)d_{x_j}^\Pi, d_{x_i}^\Pi \right\rangle = \sum_{j=0}^{i-1} (\lambda_{j+1}^- - \lambda_j^-) \langle g - d_{x_j}^\Pi, d_{x_i}^\Pi \rangle = 0,$$

where the last inequality follows from the fact that $\text{supp}(u_{x_j}) \subset \text{supp}(u_{x_i})$. This proves that $\langle x_0 + \lambda_{i-1}^- g - x_{i-1}, d_{x_{i-1}}^\Pi \rangle = 0$ for all $i \geq 1$, i.e., we only take shadow steps in TRACE. Moreover, the number of breakpoints is at most n , since $\text{supp}(u_{x_i}) \subset \text{supp}(u_{x_{i-1}}) \subset \dots \subset \text{supp}(u_{x_0})$, and thus it will take n iterations until $|\text{supp}(u_{x_i})| = 1$, at which point $d_{x_i}^\Pi = 0$, so that we reached the endpoint of the projections curve by Theorem 3. \square

D Missing Proofs for Section 4

D.1 Proof of Lemma 5

Lemma 5 (Steepest feasible descent of Shadow Steps). *Let $\mathcal{P} \subseteq \mathbb{R}^n$ be a polytope defined as in (3) and let $x \in \mathcal{P}$ with gradient $\nabla h(x)$ be given. Let y be any feasible direction at x , i.e., $\exists \gamma > 0$ s.t. $x + \gamma y \in \mathcal{P}$. Then*

$$\left\langle -\nabla h(x), \frac{d_x^\Pi}{\|d_x^\Pi\|} \right\rangle^2 = \|d_x^\Pi\|^2 \geq \left\langle d_x^\Pi, \frac{y}{\|y\|} \right\rangle^2 \geq \left\langle -\nabla h(x), \frac{y}{\|y\|} \right\rangle^2. \quad (14)$$

Proof. We prove the result using first-order optimality of projections. First, observe that using Moreau's decomposition theorem we can uniquely decompose $-\nabla h(x) = p + d_x^\Pi$ such that $\langle d_x^\Pi, p \rangle = 0$, where p is the projection of $-\nabla h(x)$ onto $N_{\mathcal{P}}(x)$. Therefore, $\langle -\nabla h(x), d_x^\Pi \rangle = \|d_x^\Pi\|^2$, which gives the first equality in (14).

We will now show that

$$\langle d_x^\Pi, y \rangle \geq \langle -\nabla h(x), y \rangle. \quad (43)$$

To do that, we recall the first-order optimality condition for $g(\lambda) = \Pi_{\mathcal{P}}(x - \lambda \nabla h(x))$ for $\lambda > 0$:

$$\langle g(\lambda) - x + \lambda \nabla h(x), z - g(\lambda) \rangle \geq 0 \quad \forall z \in \mathcal{P}.$$

Using Theorem 3, we know that there exists some scalar λ^- such that $g(\lambda) = x + \lambda d_x^\Pi$ for any $0 < \lambda < \lambda^-$. Hence, for any such $\lambda \in (0, \lambda^-)$, the first-order optimality condition becomes:

$$\langle x + \lambda d_x^\Pi - x + \lambda \nabla h(x), z - x - \lambda d_x^\Pi \rangle = \lambda \langle d_x^\Pi + \nabla h(x), z - x - \lambda d_x^\Pi \rangle \geq 0, \quad (44)$$

for all $z \in \mathcal{P}$. Note that the above equation holds for any $z \in \mathcal{P}$ and $\lambda \in (0, \lambda^-)$.

Since, $x + \gamma y \in \mathcal{P}$, it follows that $x + \bar{\lambda}y$ is also in \mathcal{P} , where $\bar{\lambda} = \min\{\lambda^-/2, \gamma\}$. Thus, since $\bar{\lambda} \in (0, \lambda^-)$ and $x + \bar{\lambda}y \in \mathcal{P}$, we can plug in $\bar{\lambda}$ for λ and $x + \bar{\lambda}y$ for z in (44) to obtain $\bar{\lambda}^2 \langle d_x^\Pi + \nabla h(x), y - d_x^\Pi \rangle \geq 0$. Thus, using the fact that $\langle -\nabla h(x), d_x^\Pi \rangle = \|d_x^\Pi\|^2$, this implies

$$\langle d_x^\Pi, y \rangle \geq \|d_x^\Pi\|^2 + \langle -\nabla h(x), y - d_x^\Pi \rangle = \langle -\nabla h(x), y \rangle$$

as claimed in (43).

We can now complete the proof using (43) as follows

$$\left\langle -\nabla h(x), \frac{d_x^\Pi}{\|d_x^\Pi\|} \right\rangle^2 = \|d_x^\Pi\|^2 \geq \left\langle d_x^\Pi, \frac{y}{\|y\|} \right\rangle^2 \geq \left\langle -\nabla h(x), \frac{y}{\|y\|} \right\rangle^2,$$

where we used Cauchy-Schwartz in the first inequality and (43) in the second inequality. \square

D.2 Proof of Lemma 6

Lemma 6 (Primal gap estimate). *Let $\mathcal{P} \subseteq \mathbb{R}^n$ be a polytope and fix any $x \in \mathcal{P}$. Consider any convex function $h : \mathcal{P} \rightarrow \mathbb{R}$ and let $x^* \in \arg \min_{x \in \mathcal{P}} h(x)$. Then, $\|d_x^\Pi\| = 0$ if and only if $x = x^*$, where $x^* = \arg \min_{x \in \mathcal{P}} h(x)$. Moreover, if h is μ -strongly convex over \mathcal{P} , then*

$$\|d_x^\Pi\|^2 \geq 2\mu(h(x) - h(x^*)). \quad (16)$$

Proof. First assume that $\|d_x^\Pi\| = 0$ so that $d_x^\Pi = 0$. Then, using Remark 1 (a), we know that $d_x^\Pi = \frac{g(\epsilon) - x}{\epsilon}$ for $\epsilon > 0$ sufficiently small. Hence, the assumption that $d_x^\Pi = 0$ implies that $g(\epsilon) = x$. Using the first-order optimality of $g(\epsilon)$ we have $\langle x - \epsilon \nabla h(x) - g(\epsilon), z - g(\epsilon) \rangle \leq 0 \quad \forall z \in \mathcal{P}$. However, since $g(\epsilon) = x$, this becomes $\langle -\epsilon \nabla h(x), z - x \rangle \leq 0 \quad \forall z \in \mathcal{P}$. This is equivalent to saying $-\nabla h(x) \in N_{\mathcal{P}}(x)$, so that $x = x^*$.

Conversely suppose that $x = x^*$. Then, it follows that $-\nabla h(x) \in N_{\mathcal{P}}(x)$. Using Lemma 1, this implies that $g(\lambda) = x$ for all $\lambda > 0$. Since $d_x^\Pi = \frac{g(\epsilon) - x}{\epsilon}$ for $\epsilon > 0$ sufficiently small, it follows that $d_x^\Pi = 0$. Thus, $\|d_x^\Pi\| = 0$ as claimed.

Now assume that h is μ strongly convex. Then, using the strong convexity inequality applied

with $y \leftarrow x + \gamma(x^* - x)$ and $x \leftarrow x$ we obtain

$$\begin{aligned} h(x + \gamma(x^* - x)) - h(x) &\geq \gamma \langle \nabla h(x_t), x^* - x \rangle + \frac{\mu\gamma^2 \|x^* - x\|^2}{2} \\ &= -\frac{\langle -\nabla h(x_t), x^* - x \rangle^2}{2\mu \|x^* - x\|^2}, \end{aligned}$$

where the second inequality is obtained by minimizing over γ . As the RHS is independent of γ , we can set $\gamma = 1$ to get

$$h(x) - h(x^*) \leq \frac{\langle -\nabla h(x_t), x^* - x \rangle^2}{2\mu \|x^* - x\|^2} \quad (45)$$

Now, applying Lemma 5 with $y = x^* - x$, completes the proof:

$$\left\langle \nabla h(x), \frac{d_x^\Pi}{\|d_x^\Pi\|} \right\rangle^2 = \|d_x^\Pi\|^2 \geq \left\langle -\nabla h(x), \frac{x^* - x}{\|x^* - x\|} \right\rangle^2 \geq 2\mu(h(x) - h(x^*)),$$

where the last inequality follows from (45). \square

D.3 Connecting Shadow-steps to Away-steps

Lemma 7 (Away-steps). *Let $\mathcal{P} \subseteq \mathbb{R}^n$ be a polytope defined as in (3) and fix $x \in \mathcal{P}$. Let $F = \{z \in \mathcal{P} : A_{I(x)}z = b_{I(x)}\}$ be the minimal face containing x . Further, choose $\delta_{\max} = \max\{\delta : x - \delta d_x^\Pi \in \mathcal{P}\}$ and consider the away point $a_x = x - \delta_{\max} d_x^\Pi$ obtained by moving maximally along the the direction of the negative shadow. Then, a_x lies in F and the corresponding away-direction is simply $x - a_x = \delta_{\max} d_x^\Pi$.*

We first recall this result from Moondra et al. [32]:

Lemma 8. *Let $\mathcal{P} = \{x \in \mathbb{R}^n : Ax \leq b\}$ be a polytope with vertex set $\mathcal{V}(\mathcal{P})$. Consider any $x \in \mathcal{P}$. Let I denote the index-set of active constraints at x and $F = \{x \in \mathcal{P} \mid A_I x = b_I\}$ be the minimal face containing x . Let $\mathcal{A}(x) := \{S : S \subseteq \mathcal{V}(\mathcal{P}) \mid x \text{ is a proper convex combination of all the elements in } S\}$ be the set of all possible active sets for x , and define $\mathcal{A} := \cup_{A \in \mathcal{A}(x)} A$. Then, we claim that $\mathcal{A} = \mathcal{V}(F)$.*

Proof of Lemma 7. First, if $\delta_{\max} = 0$, then $a_x = x$, and the result holds trivially. Now assume that $\delta_{\max} > 0$. By definition of d_x^Π , we know that $A_{I(x)} d_x^\Pi \leq 0$. Hence, since $-d_x^\Pi$ is also feasible, it follows that we must have $A_{I(x)} d_x^\Pi = 0$. This then implies that $A_{I(x)} a_x = A_{I(x)}(x - \delta_{\max} d_x^\Pi) = A_{I(x)} x = b_{I(x)}$. Thus, we have $a_x \in F$. Moreover, in the proof of the previous lemma (Lemma 8), we show that the vertices of F in fact form all possible away-steps. The result then follows. \square

E Missing Proofs for Section 5

E.1 Proof of Theorem 8

Theorem 8. *Assume that the directional derivative $d_{X(t)}^\phi$ exists for all $t \geq 0$. Then, the dynamics for mirror descent (21) are equivalent to the shadow dynamics $\dot{X}(t) = d_{X(t)}^\phi$ with the same initial*

conditions $X(0) = x^{(0)} \in \mathcal{P}$.

Proof. Consider the dynamics given in (21). Using the chain rule we know that

$$\dot{X}(t) = \frac{d}{dt} \nabla \phi^*(Z(t)) = \left\langle \nabla^2 \phi^*(Z(t)), \dot{Z}(t) \right\rangle = \left\langle \nabla^2 \phi^*(Z(t)), -\nabla h(X(t)) \right\rangle.$$

By definition, the directional derivative of $\nabla \phi^*$ with respect to the direction $-\nabla h(X(t))$ is given by

$$\nabla_{-\nabla h(X(t))}^2 \phi(Z(t)) := \lim_{\epsilon \downarrow 0} \frac{\nabla \phi^*(Z(t) - \epsilon \nabla h(X(t))) - \nabla \phi^*(Z(t))}{\epsilon} = \left\langle \nabla^2 \phi^*(Z(t)), -\nabla h(X(t)) \right\rangle,$$

(see for example [45]). Hence, using this fact and the ODE definition in (21) we have

$$\begin{aligned} \dot{X}(t) &= \left\langle \nabla^2 \phi^*(Z(t)), -\nabla h(X(t)) \right\rangle = \lim_{\epsilon \downarrow 0} \frac{\nabla \phi^*(Z(t) - \epsilon \nabla h(X(t))) - \nabla \phi^*(Z(t))}{\epsilon} \\ &= \lim_{\epsilon \downarrow 0} \frac{\nabla \phi^*(Z(t) - \epsilon \nabla h(X(t))) - X(t)}{\epsilon} \end{aligned}$$

Since ϕ is strongly convex, it is known that $\nabla \phi = (\nabla \phi^*)^{-1}$ (in particular, from the duality of ϕ and ϕ^* we know that $x = \nabla \phi^*(\tilde{x})$ if and only $\tilde{x} = \nabla \phi(x)$; see Theorem 23.5 in [45]). Moreover, by definition of the mirror descent ODE given in (21), we have $X(t) = \nabla \phi^*(Z(t))$. Using these facts we get $Z(t) = (\nabla \phi^*)^{-1}(X(t)) = \nabla \phi(X(t))$. Thus,

$$\dot{X}(t) = \lim_{\epsilon \downarrow 0} \frac{\nabla \phi^*(\nabla \phi(X(t)) - \epsilon \nabla h(X(t))) - X(t)}{\epsilon} = d_{X(t)}^\phi$$

which coincides with dynamics for moving in the shadow of the gradient given in (22). \square

E.2 Proof of Theorem 9

Theorem 9. *Let $\mathcal{P} \subseteq \mathbb{R}^n$ be a polytope and suppose that $h : \mathcal{P} \rightarrow \mathbb{R}$ is differentiable and μ -strongly convex over \mathcal{P} . Consider the shadow dynamics $\dot{X}(t) = d_{X(t)}^\Pi$ with initial conditions $X(0) = x^{(0)} \in \mathcal{P}$. Then for each $t \geq 0$, we have $X(t) \in \mathcal{P}$. Moreover, the primal gap associated with the shadow dynamics decreases as:*

$$h(X(t)) - h(x^*) \leq e^{-2\mu t} h(X(0)) - h(x^*).$$

Proof. Define $w(X(t)) := h(X(t)) - h(x^*)$. First, the fact that $X(t) \in \mathcal{P}$ for all $t \geq 0$ is guaranteed by the equivalence between the dynamics of PGD (21) and shadow dynamics asserted in Theorem 9, which by construction satisfy $X(t) \in \mathcal{P}$ for all $t \geq 0$. Now the proof for the convergence rate uses a Lyapunov argument, where we let $h(X(t))$ be our Lyapunov potential function. Using the chain rule we have

$$\frac{dw(X(t))}{dt} = \left\langle \nabla h(X(t)), \dot{X}(t) \right\rangle \tag{46}$$

$$= \left\langle \nabla h(X(t)), d_{X(t)}^\Pi \right\rangle \tag{47}$$

$$= -\|d_{X(t)}^{\Pi}\|^2 \tag{48}$$

$$\leq -2\mu w(X(t)), \tag{49}$$

where we used the fact that $\dot{X}(t) = d_{X(t)}^{\Pi}$ in (47), the fact that $\langle -\nabla h(X(t)), d_{X(t)}^{\Pi} \rangle = \|d_{X(t)}^{\Pi}\|^2$ in (48), and finally the primal gap estimate (16) in (49). Integrating both sides of the above inequality (and using Grönwall’s inequality [46]) yields the result \square

E.3 Proof of Theorem 10

Theorem 10. *Let $\mathcal{P} \subseteq \mathbb{R}^n$ be a polytope and suppose that $h : \mathcal{P} \rightarrow \mathbb{R}$ is L -smooth and μ -strongly convex over \mathcal{P} . Then the primal gap of the SHADOW-WALK algorithm decreases geometrically:*

$$(h(x^{(t+1)}) - h(x^*)) \leq \left(1 - \frac{\mu}{L}\right) (h(x^{(t)}) - h(x^*))$$

with each iteration of the SHADOW-WALK algorithm (assuming TRACE-OPT is a single step). Moreover, the number of oracle calls to shadow, in-face shadow and line-search oracles to obtain an ϵ -accurate solution is $O\left(\beta \frac{L}{\mu} \log\left(\frac{1}{\epsilon}\right)\right)$, where β is the maximum number of breakpoints of the parametric projections curve that the TRACE-OPT method visits.

Proof. Since $x^{(t+1)} := \text{TRACE}(x^{(t)}, \nabla h(x^{(t)}))$ and $\text{TRACE}(x^{(t)}, \nabla h(x^{(t)}))$ traces $g(\lambda) = \Pi_{\mathcal{P}}(x^{(t)} - \lambda \nabla h(x^{(t)}))$ until we hit the $1/L$ step size with exact line-search, it follows that $h(x^{(t+1)}) \leq h(g(1/L))$, and we are thus guaranteed to make at least as much progress per iteration as that of PGD step with a fixed-step size of $1/L$. Hence we get the same standard rate $(1 - \frac{\mu}{L})$ of decrease as PGD with fixed step size $1/L$ [33]. Moreover, the iteration complexity of the number of oracle calls stated in the theorem now follows using the above rate of decrease in the primal gap. \square

Acknowledgments.

The research presented in this paper was partially supported by the Georgia Institute of Technology ARC TRIAD fellowship and NSF grant CRII-1850182.

References

- [1] R. Freund, P. Grigas, and R. Mazumder, “An extended Frank–Wolfe method with “in-face” directions, and its application to low-rank matrix completion,” *SIAM Journal on Optimization*, vol. 27, no. 1, p. 319–346, 2015.
- [2] M. Jaggi, “Revisiting Frank-Wolfe: Projection-free sparse convex optimization,” in *Proceedings of the 30th international conference on machine learning*, 2013, pp. 427–435.
- [3] M. A. Bashiri and X. Zhang, “Decomposition-invariant conditional gradient for general polytopes with line search,” in *Advances in Neural Information Processing Systems*, 2017, p. 2687–2697.

- [4] R. Lyons and Y. Peres, *Probability on trees and networks*. Cambridge University Press, New York, 2005.
- [5] A. Joulin, K. D. Tang, and F. Li, “Efficient image and video co-localization with Frank-Wolfe algorithm,” in *Computer Vision - ECCV 2014 - 13th European Conference*, 2014, pp. 253–268.
- [6] R. K. Ahuja, T. L. Magnanti, and J. B. Orlin, *Network Flows: Theory, Algorithms, and Applications*. Prentice-Hall, Inc., 1993.
- [7] S. Fujishige and S. Isotani, “A submodular function minimization algorithm based on the minimum-norm base,” *Pacific Journal of Optimization*, vol. 7, 2009.
- [8] A. S. Nemirovski and D. B. Yudin, “Problem complexity and method efficiency in optimization,” *Wiley-Interscience, New York*, 1983.
- [9] M. Frank and P. Wolfe, “An algorithm for quadratic programming,” *Naval Research Logistics Quarterly*, vol. 3, no. 1-2, pp. 95–110, 1956.
- [10] S. Lacoste-Julien and M. Jaggi, “On the global linear convergence of Frank-Wolfe optimization variants,” in *Advances in Neural Information Processing Systems (NIPS)*, 2015, pp. 496–504.
- [11] E. Levitin and B. Polyak, “Constrained minimization methods,” *USSR Computational Mathematics and Mathematical Physics*, vol. 6, p. 1–50, 1966.
- [12] M. D. Canon and C. Cullum, “A tight upper bound on the rate of convergence of Frank-Wolfe algorithm,” *SIAM Journal on Control*, vol. 6, no. 4, p. 509–516, 1968.
- [13] G. Lan, “The complexity of large-scale convex programming under a linear optimization oracle,” *arXiv preprint arXiv:1512.06142*, 2013.
- [14] J. GuéLat and P. Marcotte, “Some comments on wolfe’s ‘away step’,” *Mathematical Programming*, vol. 35, pp. 110–119, 1986.
- [15] D. Garber and E. Hazan, “A linearly convergent variant of the conditional gradient algorithm under strong convexity, with applications to online and stochastic optimization,” *SIAM Journal on Optimization*, vol. 26, no. 3, p. 1493–1528, 2016.
- [16] D. Garber and O. Meshi, “Linear-memory and decomposition-invariant linearly convergent conditional gradient algorithm for structured polytopes,” in *Proceedings of the 30th International Conference on Neural Information Processing Systems*, 2016, p. 1009–1017.
- [17] G. Braun, S. Pokutta, D. Tu, and S. Wright, “Blended conditional gradients: the unconditioning of conditional gradients,” *arXiv preprint arXiv:1805.07311*, 2018.
- [18] G. Lan and Y. Zhou, “Conditional gradient sliding for convex optimization,” *SIAM Journal on Optimization*, vol. 26, no. 2, pp. 1379–1409, 2016.
- [19] A. Beck and S. Shtern, “Linearly convergent away-step conditional gradient for non-strongly convex functions,” *Mathematical Programming*, vol. 164, pp. 1–27, 2017.
- [20] J. Penã and D. Rodríguez, “Polytope conditioning and linear convergence of the Frank-Wolfe algorithm,” *arXiv preprint arXiv:1512.06142*, 2015.

- [21] F. Rinaldi and D. Zeffiro, “A unifying framework for the analysis of projection-free first-order methods under a sufficient slope condition,” *arXiv preprint arXiv:2008.09781*, 2020.
- [22] —, “Avoiding bad steps in Frank-Wolfe variants,” *Computational Optimization and Applications*, vol. 84, no. 1, pp. 225–264, 2023.
- [23] V. Kolmogorov, “Practical Frank-Wolfe algorithms,” *arXiv preprint arXiv:2010.09567*, 2020.
- [24] K. G. Murty and F.-T. Yu, *Linear complementarity, linear and nonlinear programming*. Citeseer, 1988, vol. 3.
- [25] G. Dantzig and R. Cottle, “Complementary pivot theory of mathematical programming,” *Mathematics of the decision sciences, part*, vol. 1, pp. 115–136, 1968.
- [26] S. Lojasiewicz, “A topological property of real analytic subsets,” *Coll. du CNRS, Les équations aux dérivées partielles*, vol. 117, no. 87-89, p. 2, 1963.
- [27] D. P. Bertsekas, *Nonlinear programming*. Athena Scientific, 1997.
- [28] G. P. McCormick and R. A. Tapia, “The gradient projection method under mild differentiability conditions,” *SIAM Journal on Control*, vol. 10, no. 1, pp. 93–98, 1972.
- [29] C. D. Meyer, *Matrix analysis and applied linear algebra*. Siam, 2000, vol. 71.
- [30] J. J. Moreau, “Décomposition orthogonale d’un espace hilbertien selon deux cônes mutuellement polaires,” *Comptes rendus hebdomadaires des séances de l’Académie des sciences*, vol. 255, pp. 238–240, 1962.
- [31] A. Carderera, J. Diakonikolas, C. Y. Lin, and S. Pokutta, “Parameter-free Locally Accelerated Conditional Gradients,” *Proceedings of ICML*, 2 2021.
- [32] J. Moondra, H. Mortagy, and S. Gupta, “Reusing combinatorial structure: Faster iterative projections over submodular base polytopes,” *Advances in Neural Information Processing Systems*, vol. 34, pp. 25 386–25 399, 2021.
- [33] H. Karimi, J. Nutini, and M. Schmidt, “Linear convergence of gradient and proximal-gradient methods under the Polyak-lojasiewicz condition,” in *European Conference on Machine Learning and Knowledge Discovery in Databases - Volume 9851*, ser. ECML PKDD 2016. Springer-Verlag, 2016, p. 795–811.
- [34] A. Beck and M. Teboulle, “Mirror descent and nonlinear projected subgradient methods for convex optimization,” *Operations Research Letters*, vol. 31, no. 3, pp. 167–175, 2003.
- [35] A. Beck, *First-order methods in optimization*. SIAM, 2017.
- [36] W. Krichene, A. Bayen, and P. L. Bartlett, “Accelerated mirror descent in continuous and discrete time,” in *Advances in Neural Information Processing Systems 28*, 2015, pp. 2845–2853.
- [37] C. W. Combettes and S. Pokutta, “Boosting Frank-Wolfe by chasing gradients,” *arXiv preprint arXiv:2003.06369*, 2020.
- [38] G. Braun, S. Pokutta, and D. Zink, “Lazifying conditional gradient algorithms,” in *International Conference on Machine Learning (ICML)*, 2017, pp. 566–575.

- [39] D. Garber, “Revisiting Frank-Wolfe for polytopes: Strict complementarity and sparsity,” *Advances in Neural Information Processing Systems*, vol. 33, 2020.
- [40] P. Dvurechensky, K. Safin, S. Shtern, and M. Staudigl, “Generalized self-concordant analysis of Frank–Wolfe algorithms,” *Mathematical Programming*, vol. 198, no. 1, pp. 255–323, 2023.
- [41] F. Pedregosa, G. Negiar, A. Askari, and M. Jaggi, “Linearly convergent Frank-Wolfe with backtracking line-search,” in *International conference on artificial intelligence and statistics*. PMLR, 2020, pp. 1–10.
- [42] L. Gurobi Optimization, “Gurobi optimizer reference manual version 9.0,” 2020, uRL: <https://www.gurobi.com/documentation/9.0/refman>.
- [43] F. Locatello, R. Khanna, M. Tschannen, and M. Jaggi, “A unified optimization view on generalized matching pursuit and Frank-Wolfe,” in *Artificial Intelligence and Statistics*. PMLR, 2017, pp. 860–868.
- [44] E. Wirth, T. Kerdreux, and S. Pokutta, “Acceleration of Frank-Wolfe algorithms with open-loop step-sizes,” in *International Conference on Artificial Intelligence and Statistics*. PMLR, 2023, pp. 77–100.
- [45] R. T. Rockafellar, *Convex analysis*. Princeton University Press, 1970.
- [46] T. H. Gronwall, “Note on the derivatives with respect to a parameter of the solutions of a system of differential equations,” *Annals of Mathematics*, pp. 292–296, 1919.